

# **NOCTURNAL LOW-LEVEL JET AND WIND CONVERGENCE EVENT IN COMPLEX TERRAIN OF EASTERN IDAHO**

Thomas A. Andretta

*State University of New York at Stony Brook*

*Stony Brook, New York*

## **Abstract**

This study documents a case of a nighttime low-level wind speed maximum (jet) and surface wind convergence zone in eastern Idaho on 2004 April 29. The data sources cited in the analysis include satellite, mesonet, radar, profiler, and forecast model archives. The occurrence of the 700 mb jet resulted in an area of snow that formed perpendicular to the valley openings of the Arco Desert along the axis of this jet. Snowfall also occurred in a region of surface wind convergence just south of the Arco Desert in the western part of the Snake River Plain (Magic Valley). This event lasted 6 hours accompanied by light to moderate snow, gusty winds, and a snowfall accumulation of several inches. University of Washington 12 km and 4 km horizontal domains of the MM5-GFS model were instrumental in simulating the jet forcing and wind convergence for this snow event. The National Weather Service (NWS) meteorologist at the Pocatello/Idaho Falls, Idaho forecast office issued timely and accurate snowfall projections for these regions. This study illustrates the importance of understanding the synoptic and mesoscale meteorological processes associated with snow events in topographic regions of different seasonal climatic variability.

## **1. Introduction**

Andretta (1999) applied Fourier filters to mean monthly precipitation normals in order to decompose the annual march (time series) of precipitation into 6 harmonic amplitude (percent) and 6 harmonic phase (month) charts. The harmonic analysis illuminated different spatial distributions in mean monthly precipitation over the complex terrain of eastern Idaho. In the Arco Desert, the second and fourth harmonics account for ~40 to 50 % and ~25 to 30 %, respectively, of the seasonal variability in annual precipitation time series. In other words, precipitation frequency and intensity are highly variable throughout the year with a tendency for stronger precipitation maxima in May and June. By comparison, the region south of the Arco Desert in the western part of the Snake River Plain (Magic Valley) is characterized by salient first harmonic precipitation maxima (~65 to 80 % of the annual variability) in December and January; smaller second harmonic precipitation maxima (~20 to 35 % of the annual variability) occur in May.

As noted by Andretta and Wojcik (2003), mean monthly climatological snowfall for observation

stations in the Arco Desert and Snake River Plain typically peaks in December and January. April and May are the spring months with the least amounts of measurable snowfall. In the Arco Desert and Magic Valley, average total snowfall for April is between 0.5 and 1.5 inches.

This study will focus on the synoptic and mesoscale conditions that led to a springtime snow event over the Arco Desert and Magic Valley in eastern Idaho. The observed snowfall amounts during the 6 hour event exceeded April climatological averages and were caused by several factors described in Section 4.

## 2. Background

### *a. Topography*

[Figure 1a](#) shows a map of the Northwest United States indicating the region of study with the red inset region highlighting the subdomain of interest. [Figure 1b](#) displays the topography map of eastern Idaho with county names and boundaries, including a topographic elevation legend. The main orographic feature in eastern Idaho is the Snake River Plain which is contoured in the shape of a concave parabola. The expansive plain is approximately 120 km wide and is oriented from southwest to northeast with a gradual increase in elevation from ~1300 m MSL over Lincoln county to ~1500 m MSL in southern Fremont county. This distance covers nearly 240 km. Andretta and Wojcik (2003) noted a 1500 m elevation contour that curves leftward in the shape of a fish hook across the upper part of the Snake River Plain. To the north and south of the Snake River Plain, there are higher basins and mountains that rise in elevation from ~1700 to 3500 m MSL. Note the finger-like valleys oriented across Custer and Butte counties that drain onto the upper part of the Snake River Plain in Bingham county. Similarly, there are north to south oriented valleys that allow winds to either drain out of or into the lower part of the Snake River Plain. Elevations rise to above 4000 m MSL in the central Idaho mountains.

[Figure 1c](#) shows the eastern Idaho domain with the outline of the Idaho National Engineering and Environmental Laboratory (INEEL) facility (black outline) and the NOAA ARL/FRD station locations (black squares) featured in this manuscript. The Arco Desert (which encompasses most of Butte county) is indicated by the region enclosed by the open blue rectangle in [Figure 1c](#). At the entrance point of the northwest side of the desert lies northwest to southeast oriented valley openings that aid in channeling of 700 mb winds, notably with the passage of cold fronts (Andretta and Hazen, 1998). In the east and south portion of the desert, the terrain is flatter and more exposed and opens onto the Snake River Plain. The Arco Desert receives 5 to 10 inches of precipitation per year or roughly half of the climatological values observed in the Snake River Plain (Andretta and Wojcik, 2003).

Scientific advances in Doppler radar, mesonets, and numerical forecast models have been critical in identifying several terrain induced mesoscale features. The topographic configuration in eastern Idaho is crucial to the development of cyclonic vortices (Andretta and Hazen, 1998), gap flow winds (Stewart et al., 2002), topographically distorted cold fronts (Steenburgh and Blazek, 2001), and post-cold frontal wind convergence zones of precipitation (Andretta, 2002). Several high-resolution data sets are discussed in this study and will be expounded in the next section of this manuscript.

### 3. Data Sources

#### *a. Satellite Data*

For satellite imagery, this study used 12 hourly data collected from NOAA GOES Northern Hemisphere Infrared imager. However, there was a data gap between 1200 UTC 2004 April 28 and 0000 UTC 2004 April 30. Thus, there were no real-time satellite images at the time of the actual snow event.

#### *b. Model Data*

The University of Washington generates high resolution model forecasts twice daily (0000 UTC and 1200 UTC) at various horizontal and vertical domains of the MM5-ETA and MM5-GFS models. These simulations are supported by the Northwest Regional Modeling Consortium. Please see this hyperlink for more information: <http://www.atmos.washington.edu/mm5rt/>. This study employed the 12 km and 4 km grids of the MM5-GFS model initialized at 0000 UTC on 2004 April 29. The choice of the MM5-GFS model was based on favorable model verification of several analyzed fields including the mean sea-level pressure, 500 mb geopotential heights and relative humidity fields, and 700 mb geopotential heights and relative humidity fields. The 12 km 700 mb vertical velocity model fields were not incorporated in the analysis due to excessively noisy output. The MM5-GFS CAPE values were zero over the region of study for all time steps of the model run suggesting negligible convective instability during the event.

#### *c. Observations*

The study used 3 real-time observational data sets. NOAA NWS METAR observations were generated every 15 minutes each hour. The Field Research Division of the Air Resources Laboratory (ARL/FRD) operates and maintains the National Oceanic and Atmospheric Administration/ Department of Energy (NOAA/DOE) mesonet comprised of 31 instrumented (15 m) towers located throughout the Snake River Plain and Arco Desert. The wind towers were utilized to analyze local changes in temperature and wind vector observations. The temporal frequency of the mesonet data was every 15 minutes each hour.

The NOAA ARL/FRD also operates and maintains a 915 MHz profiler and Radio Acoustic Sounding System (RASS) located near the mesonet site INTEC (open yellow square; [Figure 1c](#)) at an elevation of ~1500 m MSL. This wind profiler was used to measure the vertical depth of the direction and speed of the wind flow during the event. The temporal frequency of the wind profiler data was every 30 minutes each hour.

The NWS (KSFx) WSR-88D is located near Springfield, Idaho (open red circle; [Figure 1c](#)) at ~1400 m MSL. The composite reflectivity data, defined as the maximum reflectivity collected in the beam width at all elevation scans, was used to ascertain the location and intensity of the snow field. The temporal frequency of the radar data was every 10 minutes each hour.

## 4. Results

### *a. Satellite Data*

At 1200 UTC April 28, there was a cyclonic rotation of mid-level clouds denoting the 500 mb low pressure center ("L" symbol) over northern Idaho ([Figure 2a](#)). By 0000 UTC April 30, this low center had shifted slowly into northern Utah south of the Great Salt Lake with a cloud shield extending into southern Idaho ([Figure 2b](#)).

### *b. Model Data*

As indicated in [Figures 3a](#) and [3b](#), the MM5-GFS model at 0600 UTC 2004 April 29 depicted the 300 and 500 mb closed low pressure centers over southern Idaho. The elliptical symmetry of the low centers was oriented with the major axis extending from eastern Idaho into northeastern Nevada. The synoptic charts indicated that the center of these lows was situated near the Idaho-Utah-Nevada triple point or just northwest of the Great Salt Lake. On the western flank of the 300 mb low, there was a 70 to 80 knots wind speed maximum moving southward in the Arco Desert. A band of channeled absolute vorticity ([Figure 3b](#)) was present at 500 mb across the region of study. There was a relative humidity maximum of 90 to 100 % in the Snake River Plain and Arco Desert in both [Figures 3c](#) and [3d](#). The 700 mb low center in [Figure 4a](#) was located near the Great Salt Lake with the 850 low center (1425 m) over southern Idaho ([Figure 4b](#)). The 700 mb ([Figure 4a](#)) and 850 mb ([Figure 4b](#)) temperature pattern divulged a cold pool bulging from western Montana into central Idaho and the Arco Desert. This thermal "bulge" was characterized by a region of 700 mb -10 to -12 °C isotherms overlapping the desert. Furthermore, there was a 700 mb wind speed maximum of 30 to 35 knots overlapping this "bulge" of colder air. Wind velocities were high with northeast winds of 25 to 35 knots (700 mb level: [Figure 4a](#)) and 15 to 30 knots (850 mb level: [Figure 4b](#)) across the entire desert accompanied by a weak (1010 mb) surface cyclone ([Figure 4c](#)). As [Figure 4d](#) indicates, no precipitation was indicated in the model at this time step.

At 0900 UTC, the 300 mb and 500 mb closed low pressure centers remained nearly stationary ([Figures 5a](#) and [5b](#)). Northerly winds of 70 to 80 knots at 300 mb persisted across the desert. A well-defined band of synoptic-scale 500 mb absolute vorticity continued in the channeled northeast flow aloft ([Figure 5b](#)). The moisture content remain high with 90 to 100 % relative humidity at 500 mb ([Figure 5c](#)) and 700 mb ([Figure 5d](#)). Both the 700 mb ([Figure 6a](#)) and 850 mb ([Figure 6b](#)) low pressure centers were positioned over the Great Salt Lake. The thermal "bulge" persisted with colder air of -11 to -13°C at 700 mb ([Figure 6a](#)) seeping into the Arco Desert from western Montana and a 700 mb wind maximum (jet) of 25 to 35 knots. The 850 mb chart in [Figure 6b](#) indicated surface winds of 20 to 25 knots. The persistence of the strong 700 mb and 850 mb flow may have been associated with the longevity of the thermal "bulge" as colder air accelerated the ambient wind field. Even more interesting, there was evidence of surface wind convergence in the 10 m wind fields located south of the Arco Desert in the western part of the Snake River Plain (Magic Valley) ([Figure 6c](#)). As illustrated in [Figure 6d](#), there were several areas of precipitation that formed along the central valley openings in the Arco Desert with generally 0.04 to 0.08 of an inch of liquid precipitation (0.5 to 1.0 inches of equivalent snowfall) estimated by the model between 0600 and 0900 UTC. Precipitation amounts (0.02 to 0.08 of an inch) also occurred in the highlands south of the Snake River Plain

near the Idaho-Nevada border and along the eastern slopes of the plain.

The MM5-GFS model forecasted more changes at 1200 UTC. The low pressure centers at 300 mb and 500 mb drifted slowly into north central Utah ([Figures 7a](#) and [7b](#)). Relative humidities remained high with values between 80 and 95 % at both 500 mb in [Figure 7c](#) and 700 mb in [Figure 7d](#). The wind flow had decreased to 20 to 30 knots across the Arco Desert at both 700 mb and 850 mb ([Figures 8a](#) and [8b](#)). The region of surface wind convergence south of the Arco Desert noted earlier at 0900 UTC had weakened considerably ([Figure 8c](#)). Model precipitation estimates ([Figure 8d](#)) of generally 0.04 to 0.08 of an inch of liquid precipitation (0.5 to 1.0 inches of equivalent snowfall) occurred between 0900 and 1200 UTC and were aligned along the valley openings in the Arco Desert. Areas of precipitation (0.02 to 0.08 of an inch) persisted over the highlands south of the Snake River Plain.

### *c. Observations*

[Figure 9](#) shows the NOAA ARL/FRD RASS wind profiler and mesonet analysis at 0700 UTC. The wind profiler indicated the northeast flow through a deep layer with a 38 mph wind speed maximum at ~6000 ft AGL ([Figures 9a](#) and [9b](#)). This low-level jet corresponded with the 700 mb level and matched up well with the MM5-GFS results. The mesonet data ([Figure 9c](#)) was also particularly revealing. WSR-88D KSFY composite reflectivity data indicated a ring-shaped field of light to moderate snow across parts of the Snake River Plain (e.g., KRXE: Rexburg) and Arco Desert. These echoes were situated along the northern side of the 700 mb low as indicated by the MM5-GFS model. The most intense echoes (25 to 35 dBZ) occurred perpendicular to the valley openings in the Arco Desert and along the axis of the 700 mb jet. Surface temperatures were in the 30 to 35 °F across most of the domain although there were colder temperatures across Clark and Fremont counties associated with the seepage of cold air from western Montana, coinciding with the MM5-GFS location of the thermal "bulge". The 10 m winds drained out of the north in most instances in the Snake River Plain and Arco Desert. However, there was some evidence of a light easterly wind at mesonet stations in Lincoln, Minidoka, and Power counties. This flow was intercepted by a light north to northwest flow at mesonet stations just north and west of Blaine county as depicted in the MM5-GFS model. Thus, an area of mesoscale surface wind convergence had developed downwind of the Arco Desert and was located south of the low-level jet axis.

[Figure 10](#) illustrates the NOAA ARL/FRD RASS wind profiler and mesonet analysis at 0900 UTC. The sounding indicated the northeast flow near the surface ([Figure 10a](#)) with 34 mph wind speed maxima at ~3800 ft AGL and ~7000 ft AGL ([Figure 10b](#)). The vertical wind profile displayed a slowly veering wind profile with north winds near the surface shifting to east winds aloft. The WSR-88D KSFY composite reflectivity data ([Figure 10c](#)) showed a large circular field of echoes stretching from the upper part of the Snake River Plain to the Arco Desert. Light to moderate snow (30 to 35 dBZ) was falling across the Snake River Plain and Arco Desert. The higher reflectivities (35 dBZ) were aligned with the valley openings suggesting low-level lift induced by the presence of the 700 mb jet. Surface temperatures persisted in the ranges at 0900 UTC consistent with the location of the thermal "bulge". The mesoscale surface wind convergence signature noted at 0600 UTC persisted across Power and Minidoka counties. This feature was resolved favorably by the MM5-GFS model. The radar reflectivities in the mesoscale convergence zone were in the 15 to 25 dBZ band with the highest echo returns over Minidoka county.

[Figure 11](#) displays the NOAA ARL/FRD RASS wind profiler and mesonet analysis at 1130 UTC. The wind profiler indicated the north to east flow ([Figure 11a](#)) through a deep layer with 32 mph wind speed maxima at ~4000 ft AGL and ~11000 ft AGL ([Figure 11b](#)). The north winds at surface reporting stations had progressed into the Power and Minidoka counties and mixed out the mesoscale surface wind convergence zone. The decay of this wind convergence field followed the forecast in the MM5-GFS model. The WSR-88D KSFY composite reflectivity data ([Figure 11c](#)) indicated a decrease in both the intensity and coverage of the echoes versus 3 hours earlier. Radar reflectivities had diminished to 15 to 25 dBZ over the Snake River Plain and Arco Desert. After 1200 UTC, the radar echoes dissipated completely in these regions, signaling an end to the snow event.

#### *d. Weather Forecast and Verification*

Based on the trends in the MM5-GFS model and observations, the NWS meteorologist at the Pocatello/Idaho Falls, Idaho forecast office augmented the automated text forecast for the Arco Desert and western part of the Snake River Plain (Magic Valley) to include a snow accumulation of 1 to 3 inches during the early morning hours between 0800 and 1400 UTC. This decision proved to be very timely and accurate. [Figure 12](#) shows the total observed snowfall amounts in these regions. Weather spotters indicated blowing snow in gusty winds with an accumulation of 1 to 3 inches at locations downwind of the valley openings and near the 700 mb jet axis. The recorded snowfall amounts across the Magic Valley were a trace to 2 inches with the highest amounts occurring across parts of Minidoka county in the vicinity of the surface wind convergence zone.

## **5. Conclusions**

This study documented a case of a nighttime low-level wind speed maximum (jet) and surface wind convergence zone in eastern Idaho on 2004 April 29. The data sources cited in the analysis included satellite, mesonet, radar, profiler, and forecast model archives. The occurrence of the 700 mb jet resulted in an area of snow that formed perpendicular to the valley openings of the Arco Desert along the axis of this jet. Snowfall also occurred in a region of surface wind convergence just south of the Arco Desert in the western part of the Snake River Plain (Magic Valley). This event lasted 6 hours accompanied by light to moderate snow, gusty winds, and a snowfall accumulation of several inches. University of Washington 12 km and 4 km horizontal domains of the MM5-GFS model were instrumental in simulating the jet forcing and wind convergence for this snow event.

The National Weather Service (NWS) meteorologist at the Pocatello/Idaho Falls, Idaho forecast office analyzed real-time and prognostic data sets, adjusting the automated text forecast generated from model grids to add snowfall amounts consistent with the meteorological conditions during the early morning hours of the event. These adjustments proved timely and accurate relative to snowfall observations and model estimates. This study illustrates the importance of understanding the synoptic and mesoscale meteorological processes associated with snow events in topographic regions of different seasonal climatic variability.

## 6. References

- Andretta, T. A., and D. S. Hazen, 1998: Doppler Radar Analysis of a Snake River Plain Convergence Event. *Wea. Forecasting*, **13:2**, 482-491.
- Andretta, T. A., 1999: Harmonic Analysis of Precipitation Data in Eastern Idaho. *Natl. Wea. Dig.*, **23:1-2**, 31-40.
- Andretta, T. A., 2002: Climatology of the Snake River Plain Convergence Zone. *Natl. Wea. Dig.*, **26:3, 4**, 37-51.
- Andretta T. A., and W. Wojcik, 2003: Prediction of Heavy Snow Events in the Snake River Plain Using Pattern Recognition and Regression Techniques, Idaho. NWS-WR TM 268.
- Steenburgh, W. J., and T. R. Blazek, 2001: Topographic Distortion of a Cold Front over the Snake River Plain and Central Idaho Mountains. *Wea. Forecasting*, **16:3**, 301-314.
- Stewart, J. W., C. D. Whiteman, W. J. Steenburgh, and X. Bian, 2002: A Climatological Study of Thermally Driven Wind Systems of the U.S. Intermountain West. *Bull. Amer. Meteor. Soc.*, **83:5**, 699-708.

## Acknowledgements

The author wishes to thank the National Climatic Data Center for the NWS METAR observations and WSR-88D radial data from the KSFX site. A special thanks to the NOAA/DOE for use of the ARL/FRD mesonet and RASS wind profiler data featured in this study. The data fields used in the 12 km and 4 km horizontal domains of the MM5-GFS model were garnered from the electronic online archives of the University of Washington. Finally, the author would like to thank several reviewers for suggestions to improve the quality of this manuscript.

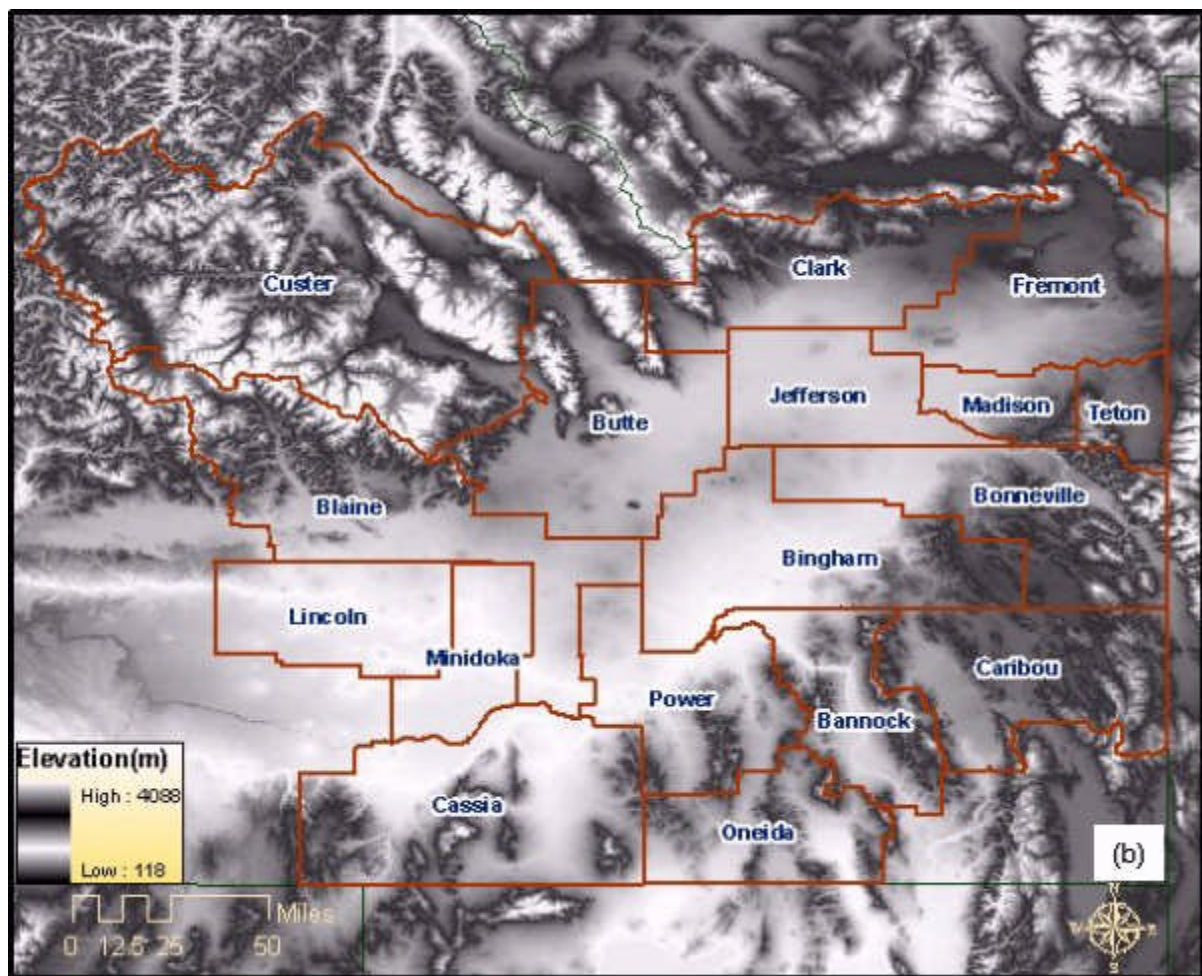
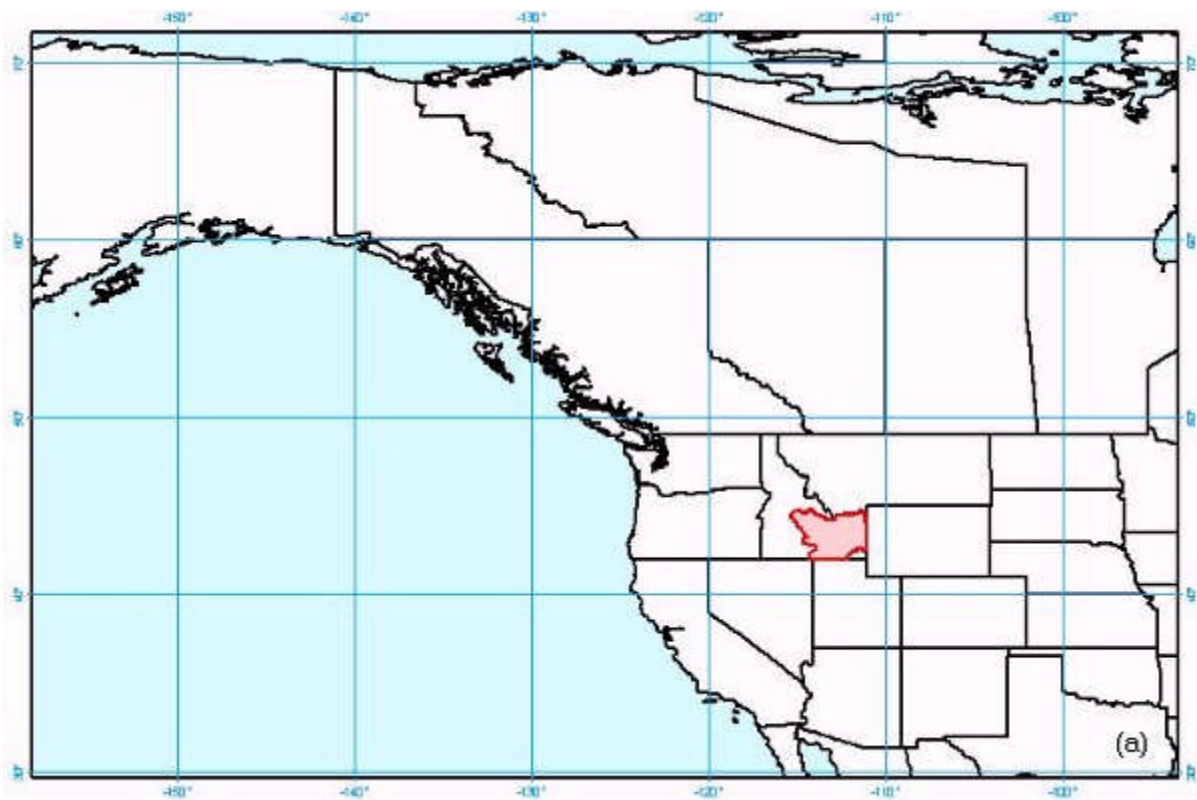
## Author

Thomas Andretta received his Bachelor of Science (1988) and Master of Science (1991) degrees in Atmospheric Science at the State University of New York (SUNY) at Stony Brook. He served as a meteorologist intern at the NWS office in Lake Charles, LA from May 1993 to April 1995 and as a staff meteorologist at the NWS office in Pocatello, ID between April 1995 and May 2005.

Mr. Andretta has lead authored two journal papers on the Snake River Plain Convergence Zone (SPCZ); he has also published other studies on annual precipitation time series, heavy snowfall synoptic patterns, and tornado climatology of eastern Idaho. His interests include boundary layer meteorology in complex terrain, fog physics, mesoscale precipitation processes, snowfall climatology, and tornado climatology. He enjoys designing meteorological applications on

Windows and Linux computer platforms.





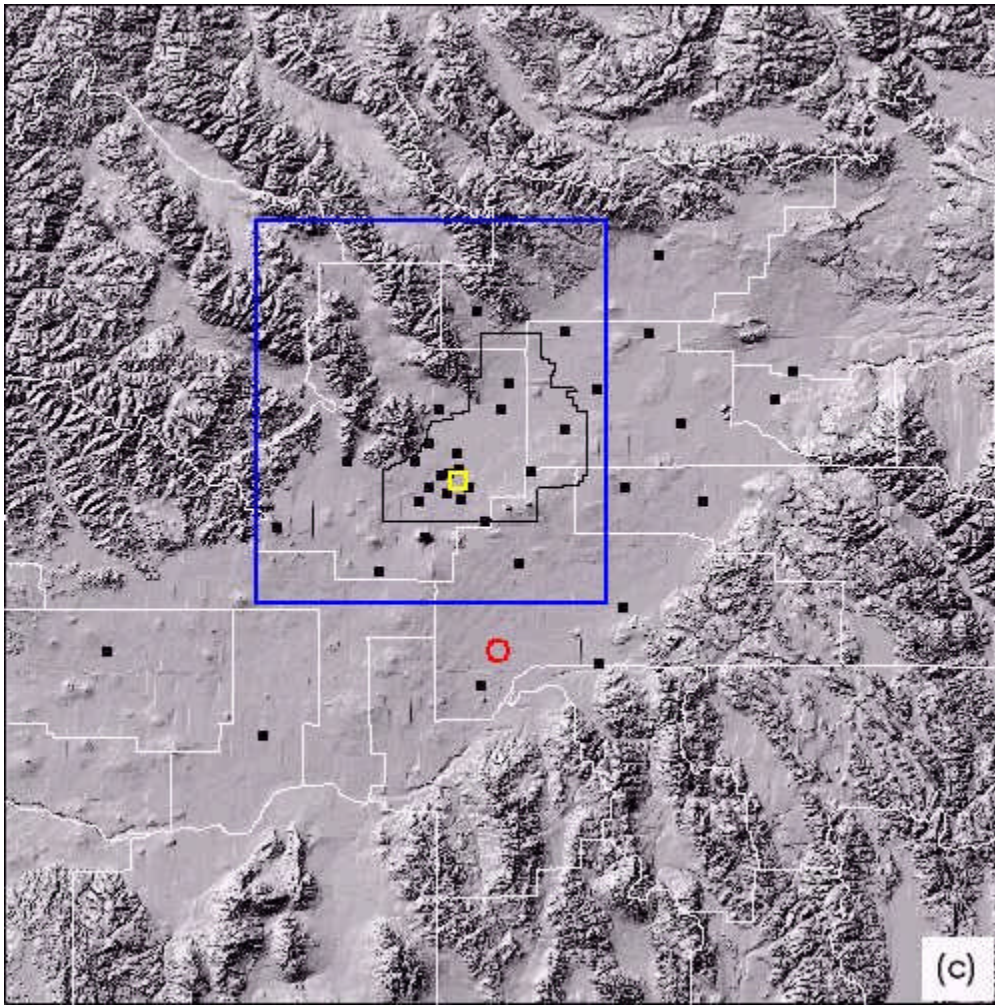


Figure 1: (a) Map of Northwest United States with inset (red) region of study  
(b) Eastern Idaho domain with county outlines and names  
(c) Eastern Idaho domain with geographical references (see text)



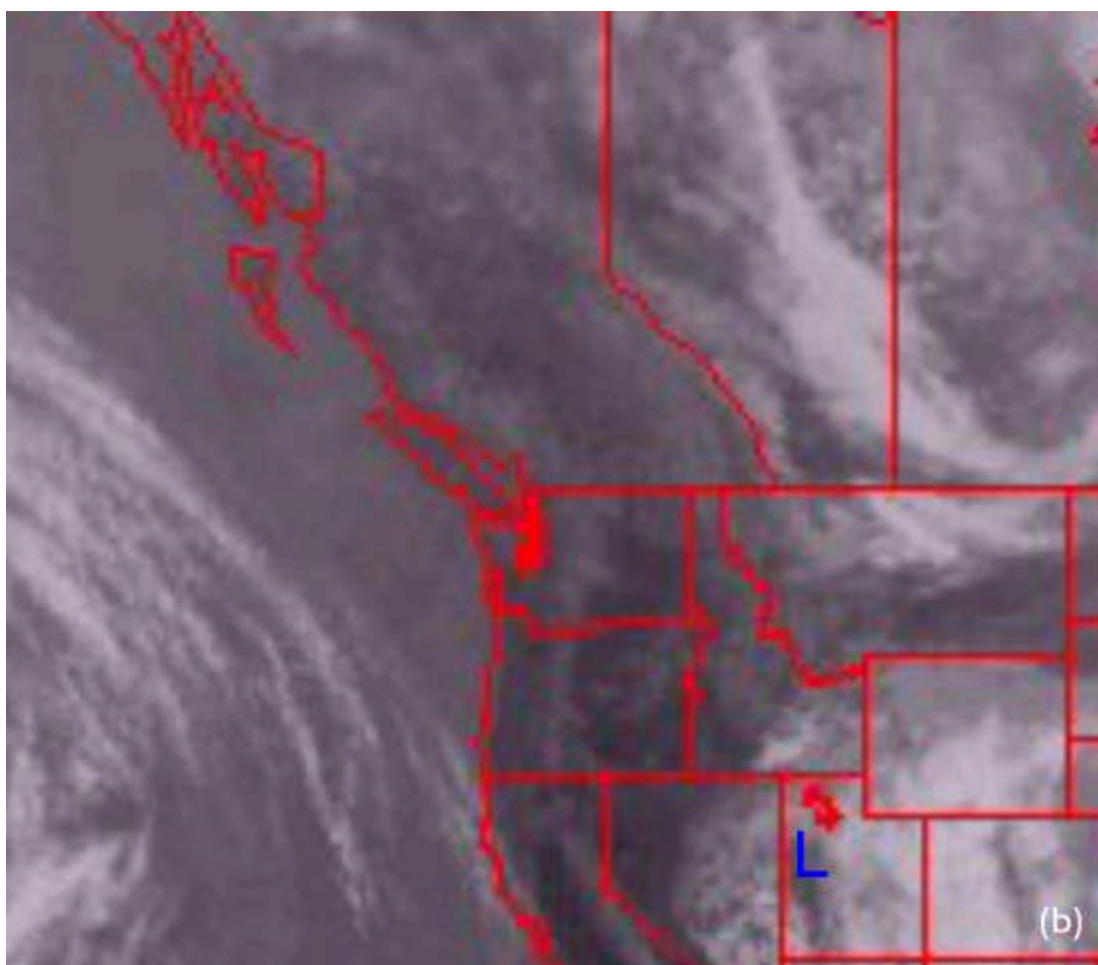
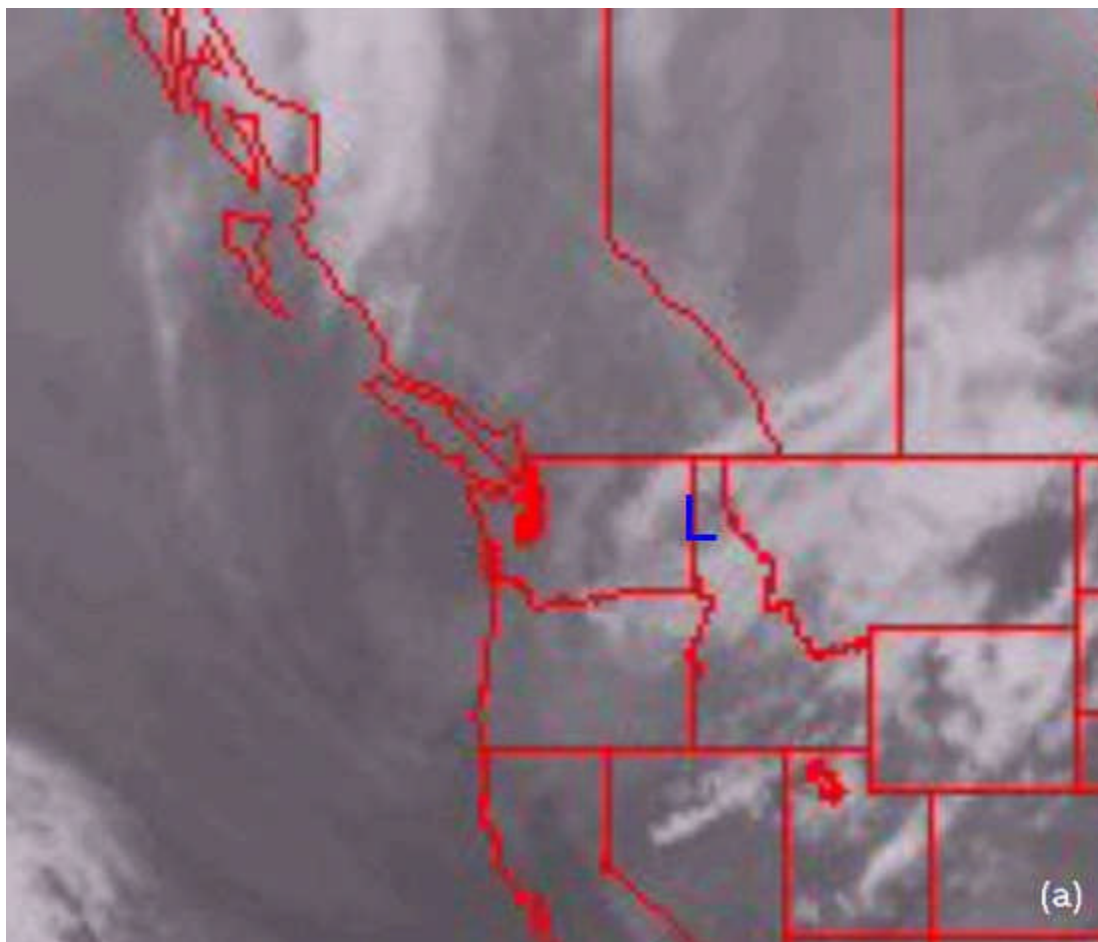
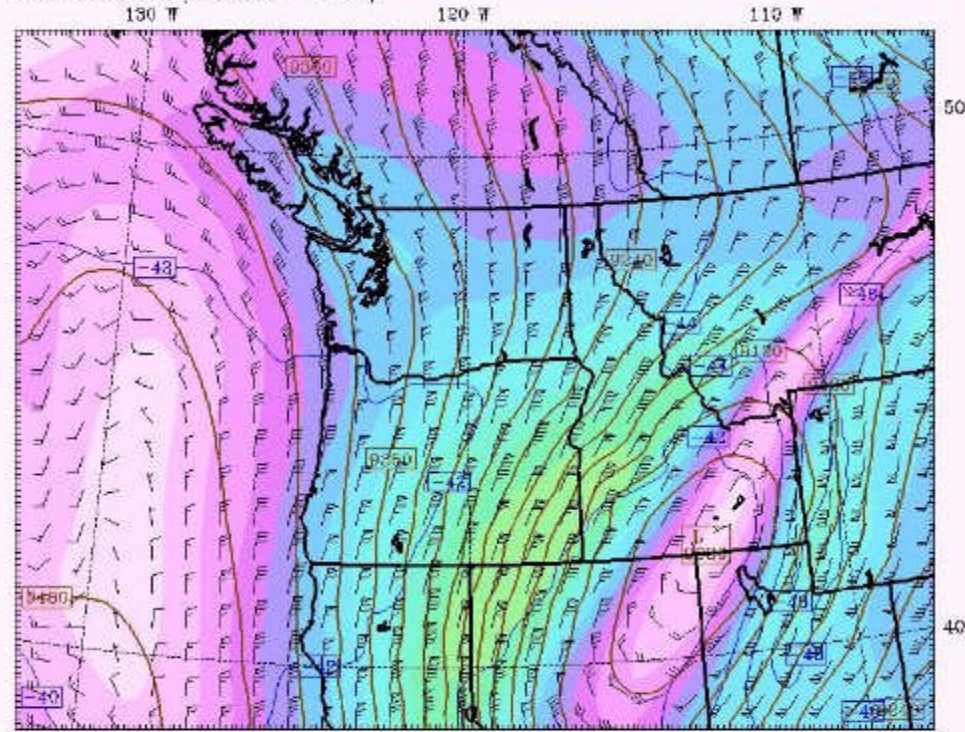


Figure 2: (a) NOAA GOES Infrared Satellite: 1200 UTC 2004 April 28  
(b) NOAA GOES Infrared Satellite: 0000 UTC 2004 April 30

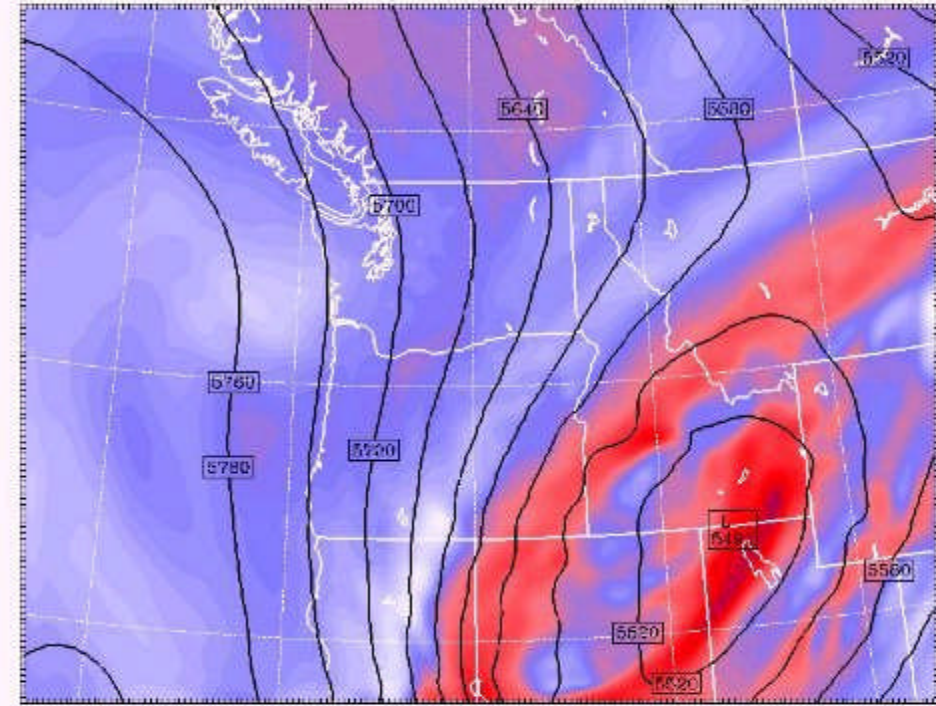


UW MM5-GFS 12km Domain  
 Init: 00 UTC Thu 29 Apr 04  
 Post: 6 h  
 Valid: 06 UTC Thu 29 Apr 04 (23 PDT Wed 28 Apr 04)  
 300 mb wind speed (m/s)  
 Temperature at 300mb (°C)  
 Geopotential Height at 300mb (m)  
 Wind at 300mb (full barb = 10kts)



CONTOURS: UNITS-m LOW- 9060.0 HIGH- 9480.0 INTERVAL- 30.000  
 CONTOURS: UNITS-°C LOW- -43.000 HIGH- 55.000 INTERVAL- 2.0000  
 Model info: V3.8.2 Kain-Frac MRF PBL Reissner 2 12 km 37 levels 39 sec (a)

UW MM5-GFS 12km Domain  
 Init: 00 UTC Thu 29 Apr 04  
 Post: 6 h  
 Valid: 06 UTC Thu 29 Apr 04 (23 PDT Wed 28 Apr 04)  
 Absolute vorticity  
 at pressure = 500 hPa  
 Geopotential Height at 500mb (m)



CONTOURS: UNITS-m LOW- 5490.0 HIGH- 5790.0 INTERVAL- 30.000  
 Model info: V3.8.2 Kain-Frac MRF PBL Reissner 2 12 km 37 levels 39 sec (b)



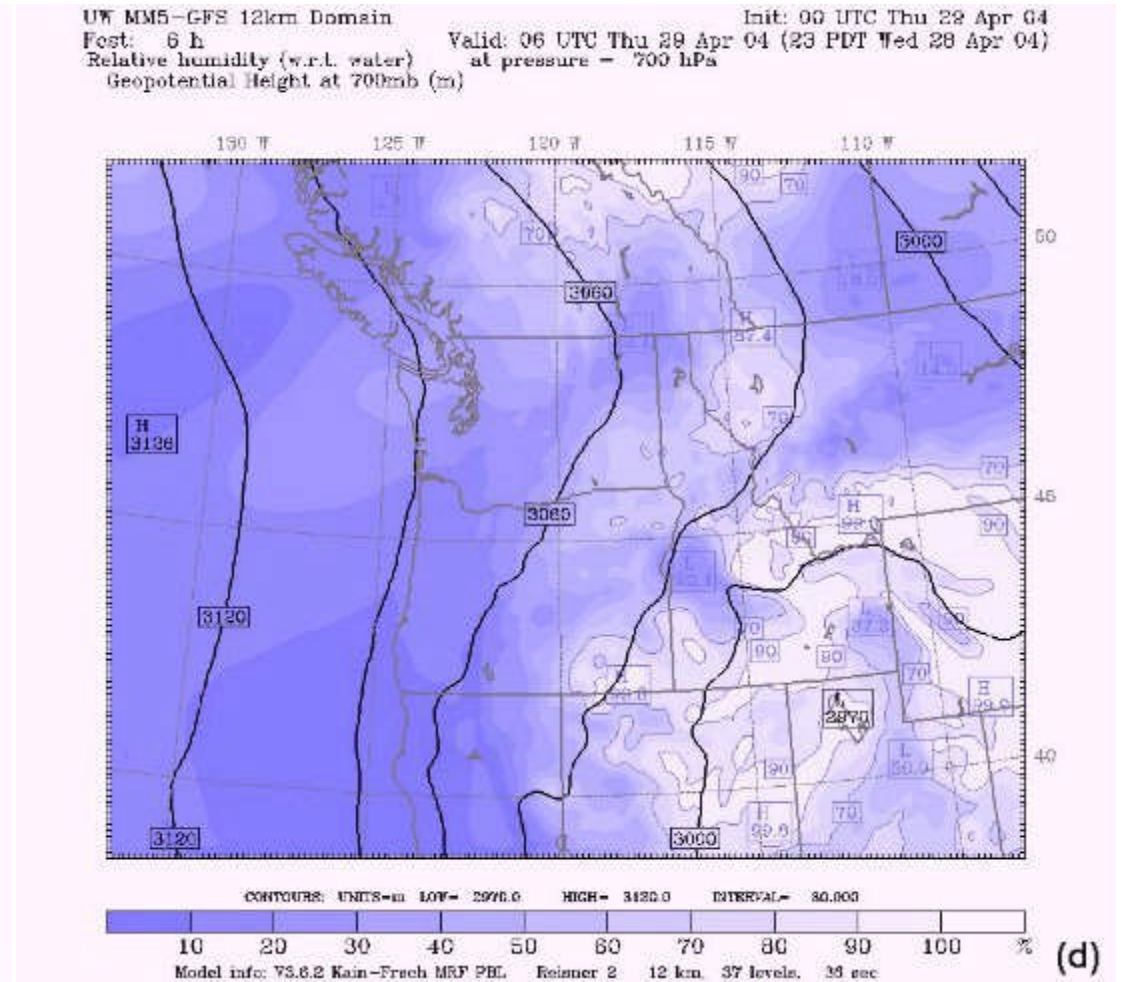
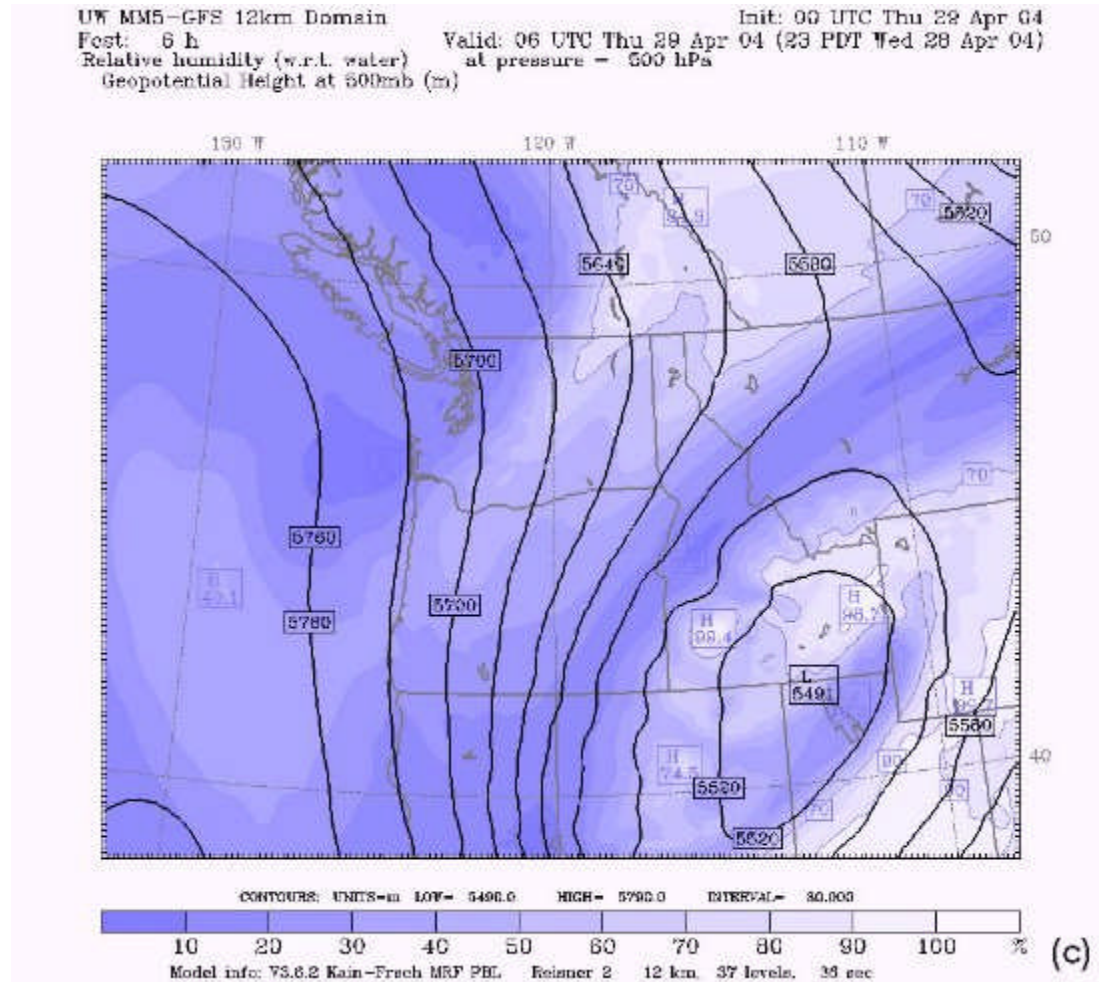
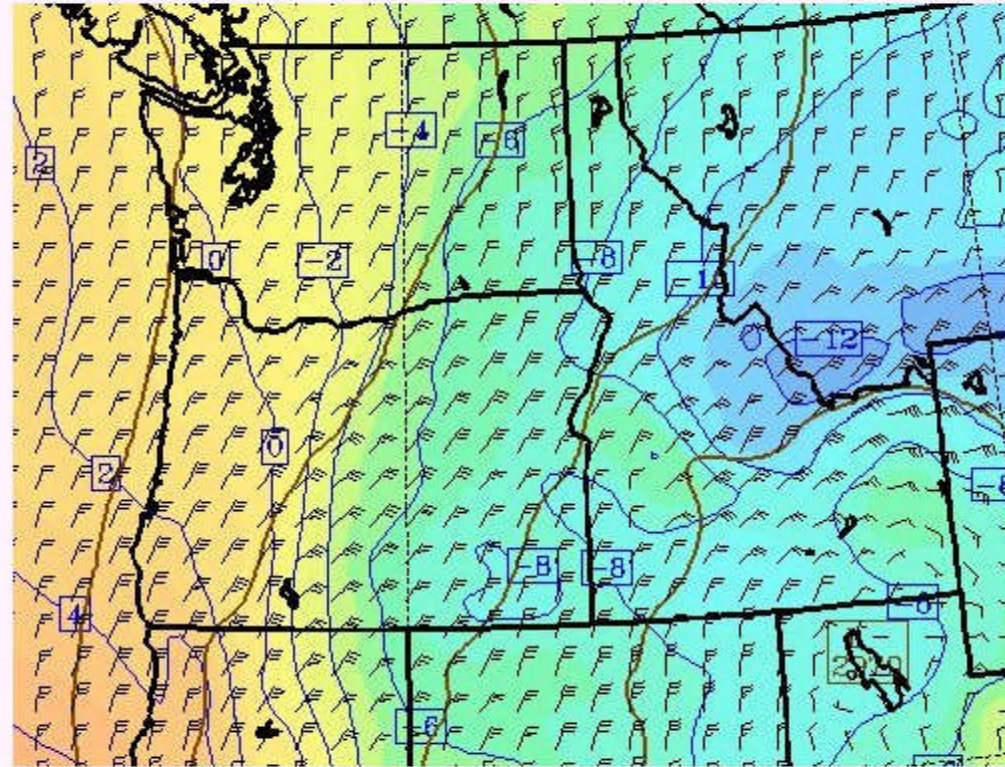


Figure 3: (a) MM5-GFS 300 mb wind speed ( $\text{m s}^{-1}$ ), temperature ( $^{\circ}\text{C}$ ), geopotential height (m), and wind (kt)  
 (b) MM5-GFS 500 mb absolute vorticity ( $\text{s}^{-1}$ ) and geopotential height (m)  
 (c) MM5-GFS 500 mb relative humidity (%) and geopotential height (m)  
 (d) MM5-GFS 700 mb relative humidity (%) and geopotential height (m)



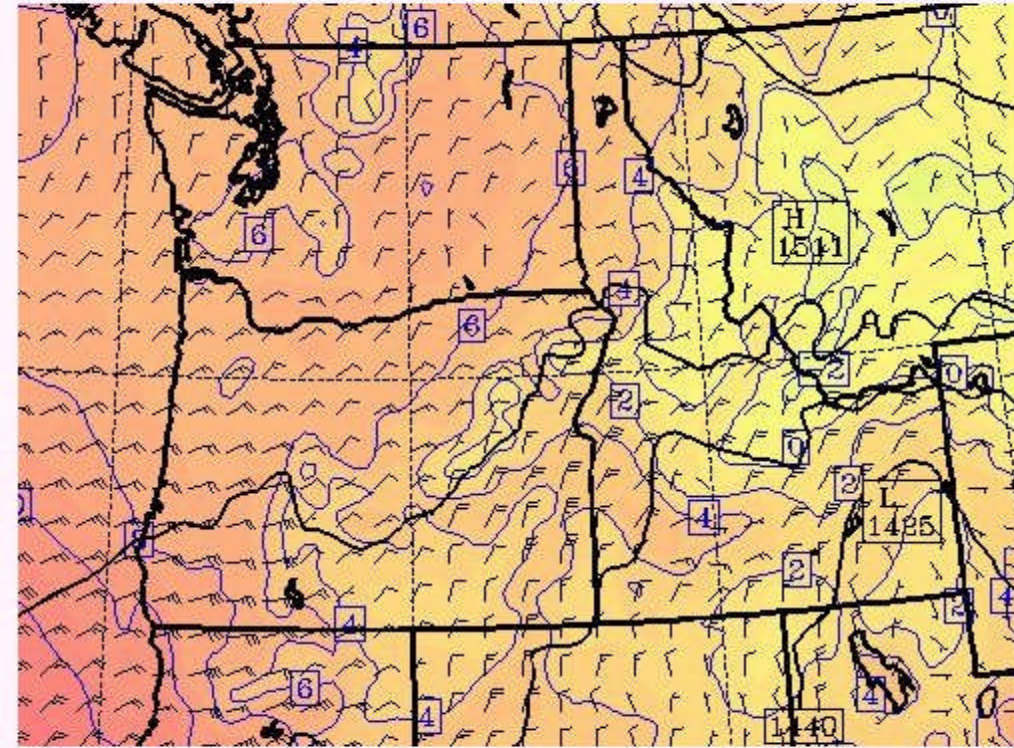
UW MM5-GFS 12km Domain      Init: 00 UTC Thu 28 Apr 04  
 Post: 6 h      Valid: 06 UTC Thu 29 Apr 04 (23 PDT Wed 28 Apr 04)  
 Temperature at 700mb (°C)  
 Geopotential Height at 700mb (m)  
 Wind at 700mb (full barb = 10kts)



CONTOURS: UNITS-m LOV- 5976.0 HIGH- 3185.0 INTERVAL- 30.000  
 CONTOURS: UNITS=°C LOW- -12.000 HIGH- 6.0000 INTERVAL- 2.0000  
 Model info: V3.8.2 Kain-Franch MRF PBL Reisman 2 12 km, 37 levels, 35 sec

(a)

UW MM5-GFS 12km Domain      Init: 00 UTC Thu 28 Apr 04  
 Post: 6 h      Valid: 06 UTC Thu 29 Apr 04 (23 PDT Wed 28 Apr 04)  
 Temperature at 850mb (°C)  
 Geopotential Height at 850mb (m)  
 Wind at 850mb (full barb = 10kts)



CONTOURS: UNITS-m LOV- 1416.0 HIGH- 1530.0 INTERVAL- 30.000  
 CONTOURS: UNITS=°C LOW- -4.0000 HIGH- 14.000 INTERVAL- 2.0000  
 Model info: V3.8.2 Kain-Franch MRF PBL Reisman 2 12 km, 37 levels, 35 sec

(b)



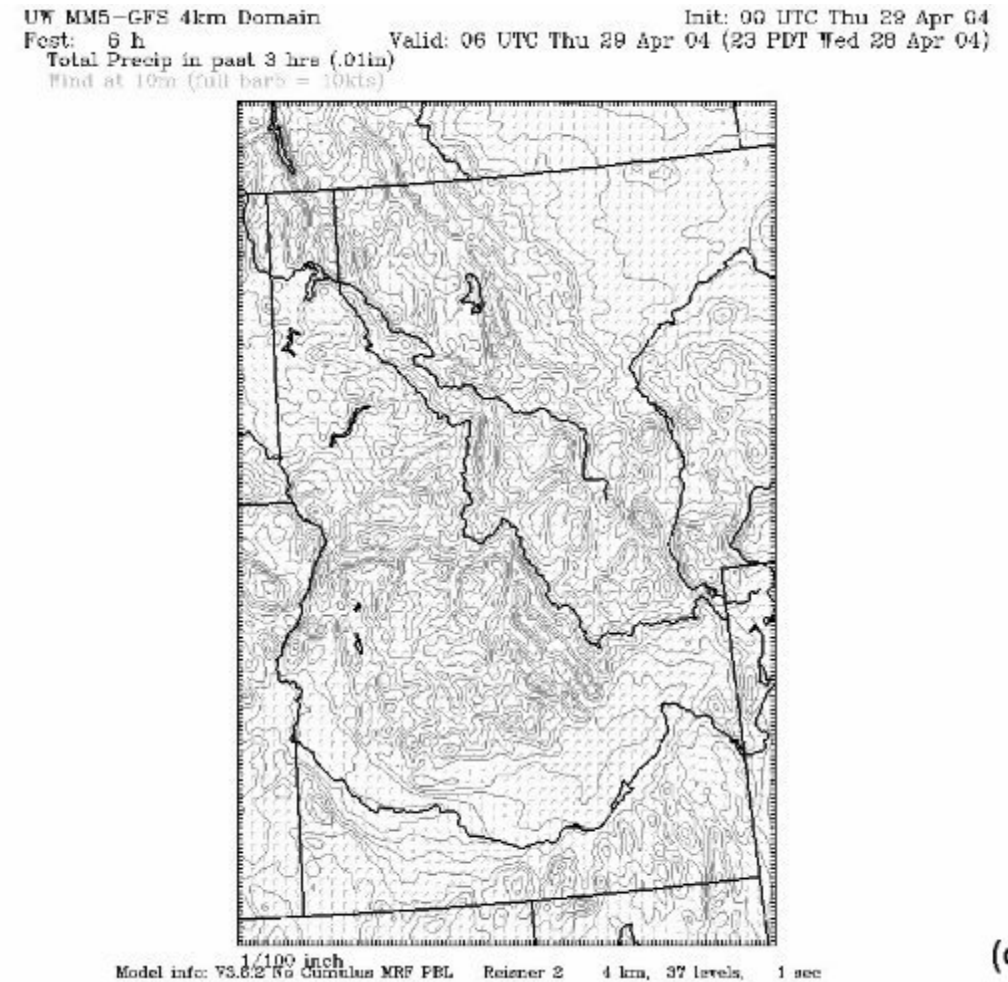
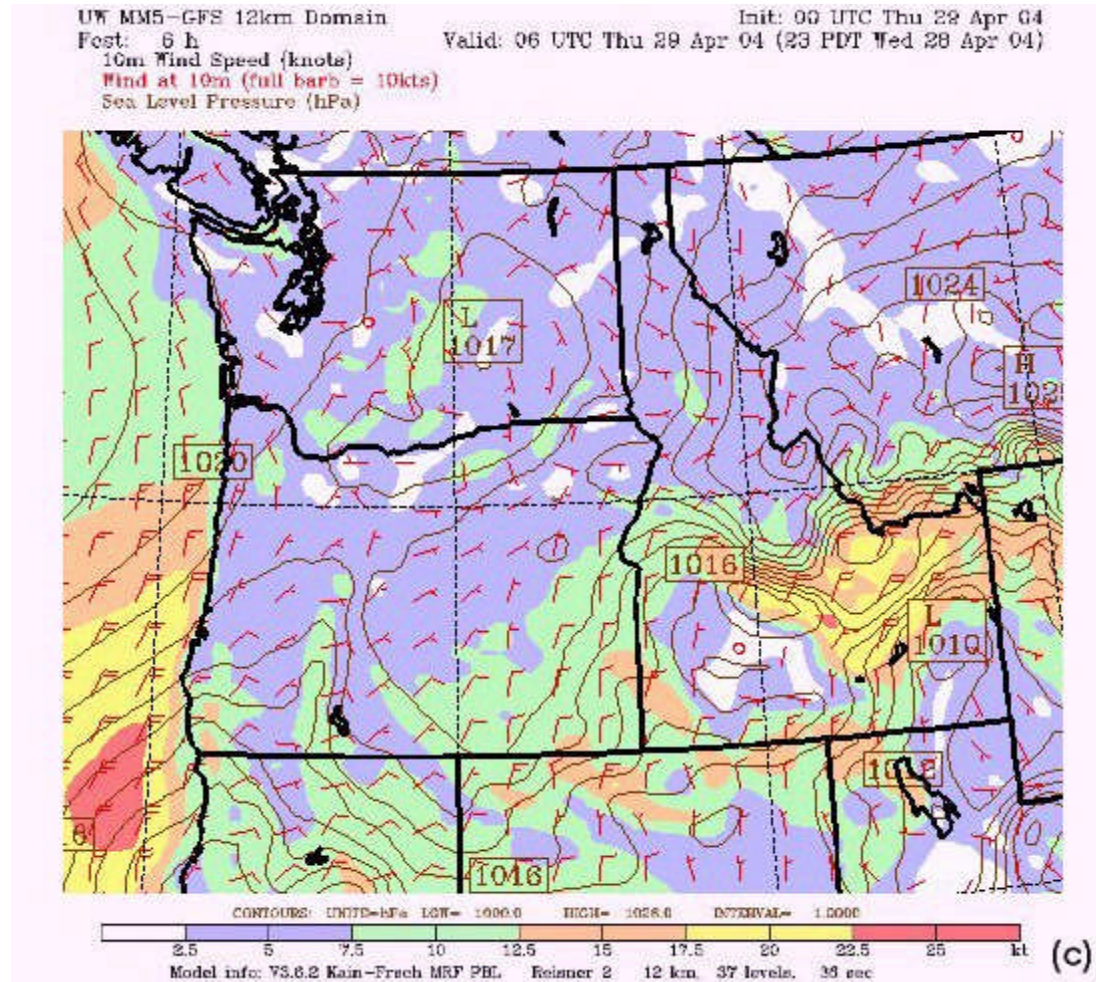
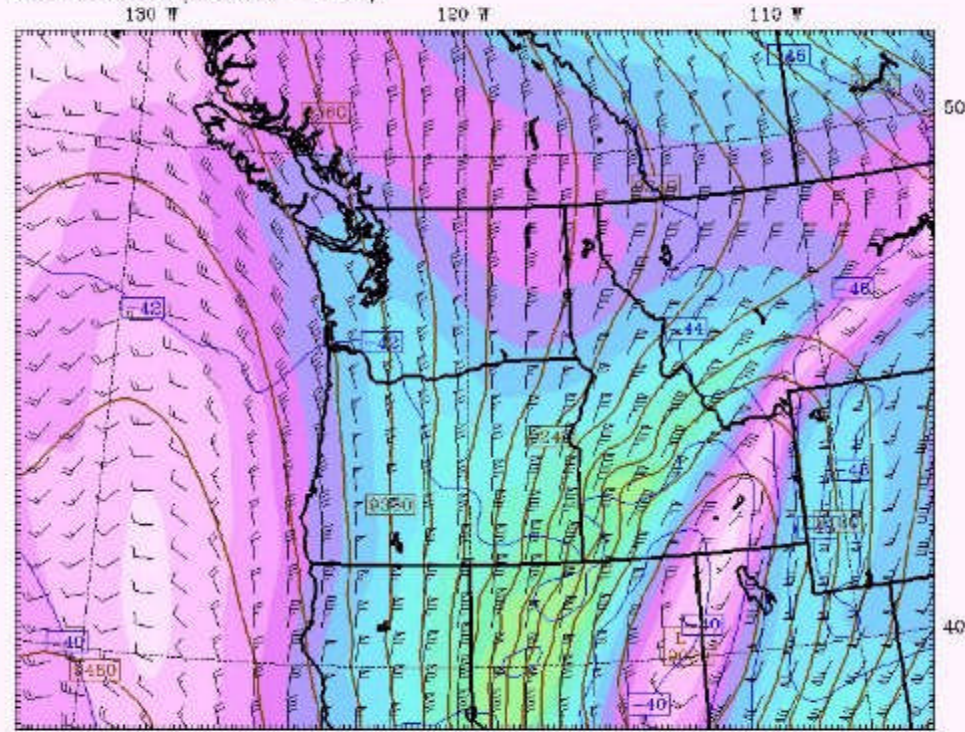


Figure 4: (a) MM5-GFS 700 mb temperature ( $^{\circ}\text{C}$ ), geopotential height (m), and wind speed (kt)  
 (b) MM5-GFS 850 mb temperature ( $^{\circ}\text{C}$ ), geopotential height (m), and wind speed (kt)  
 (c) MM5-GFS 10 m wind speed (kt) and mean sea-level pressure (hPa)  
 (d) MM5-GFS total precipitation in past 3 hours (in) and 10 m wind speed (kt)



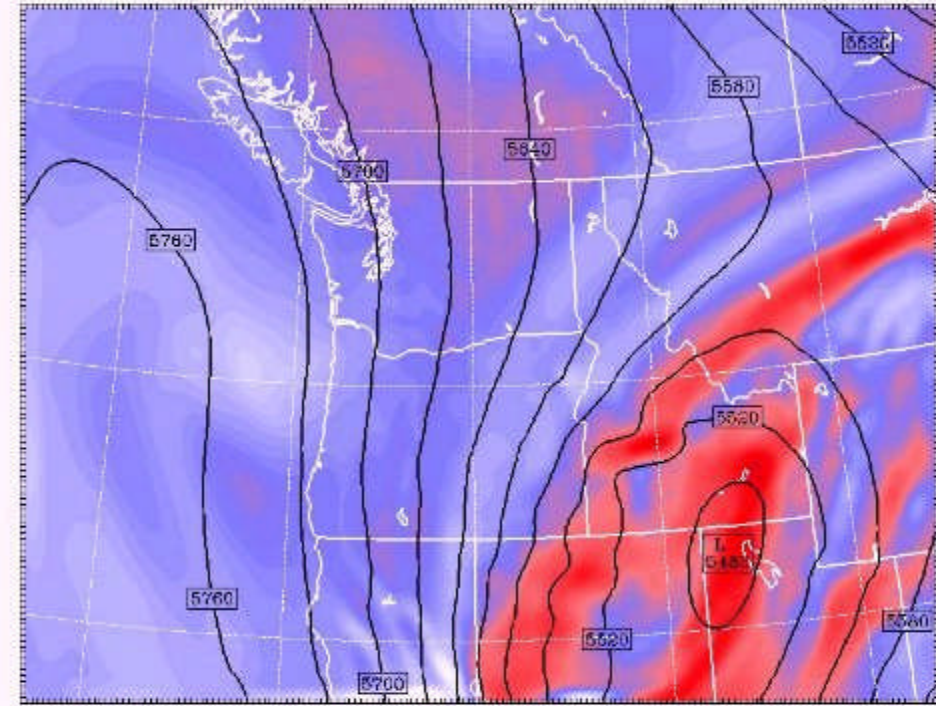
UW MM5-GFS 12km Domain Init: 00 UTC Thu 29 Apr 04  
 Post: 9 h Valid: 09 UTC Thu 29 Apr 04 (02 PDT Thu 29 Apr 04)  
 300 mb wind speed (m/s)  
 Temperature at 300mb (°C)  
 Geopotential Height at 300mb (m)  
 Wind at 300mb (full barb = 10kts)



Model info: V3.6.2 Kain-Franch MRF PBL Reissner 2 12 km 37 levels 39 sec

(a)

UW MM5-GFS 12km Domain Init: 00 UTC Thu 29 Apr 04  
 Post: 9 h Valid: 09 UTC Thu 29 Apr 04 (02 PDT Thu 29 Apr 04)  
 Absolute vorticity  
 Geopotential Height at 500mb (m)



Model info: V3.6.2 Kain-Franch MRF PBL Reissner 2 12 km 37 levels 39 sec

(b)



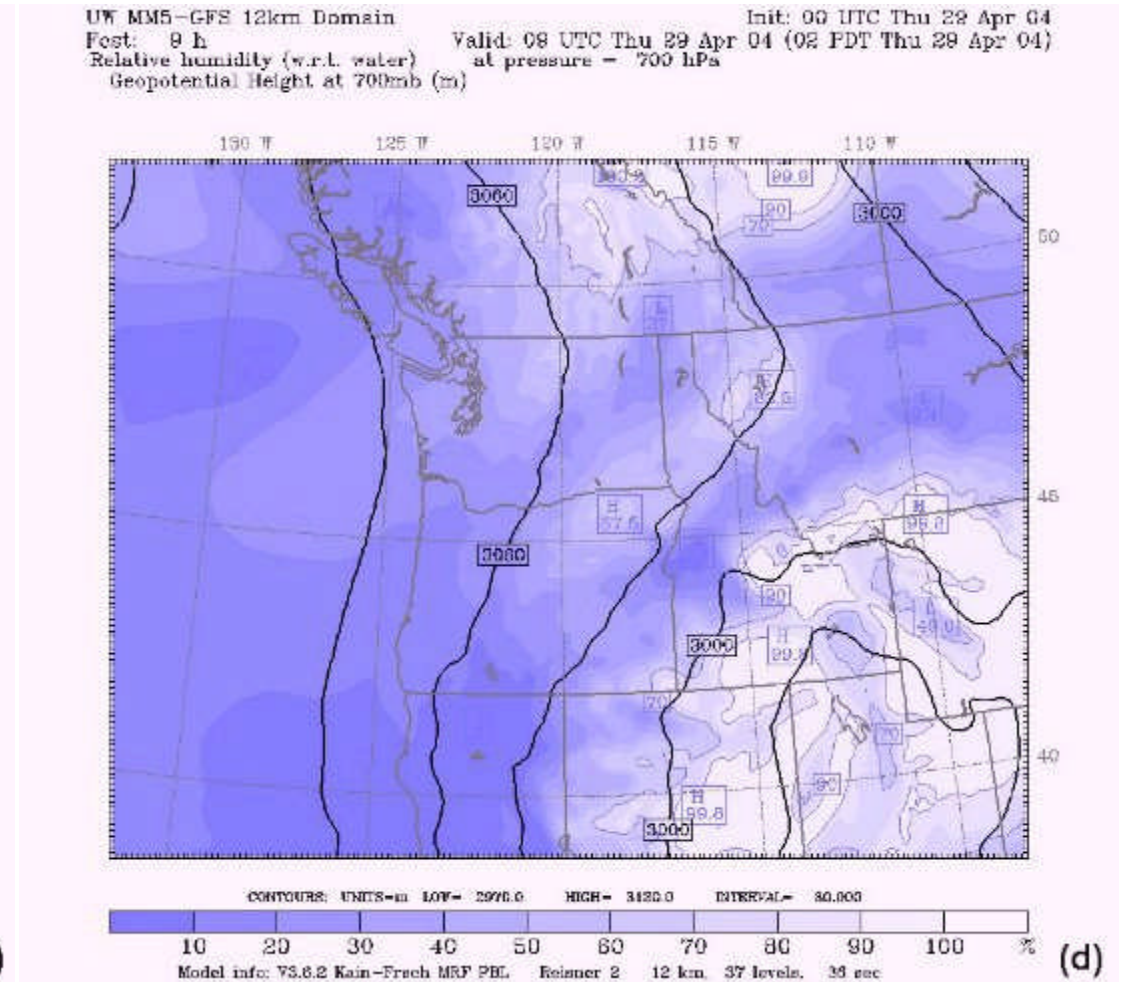
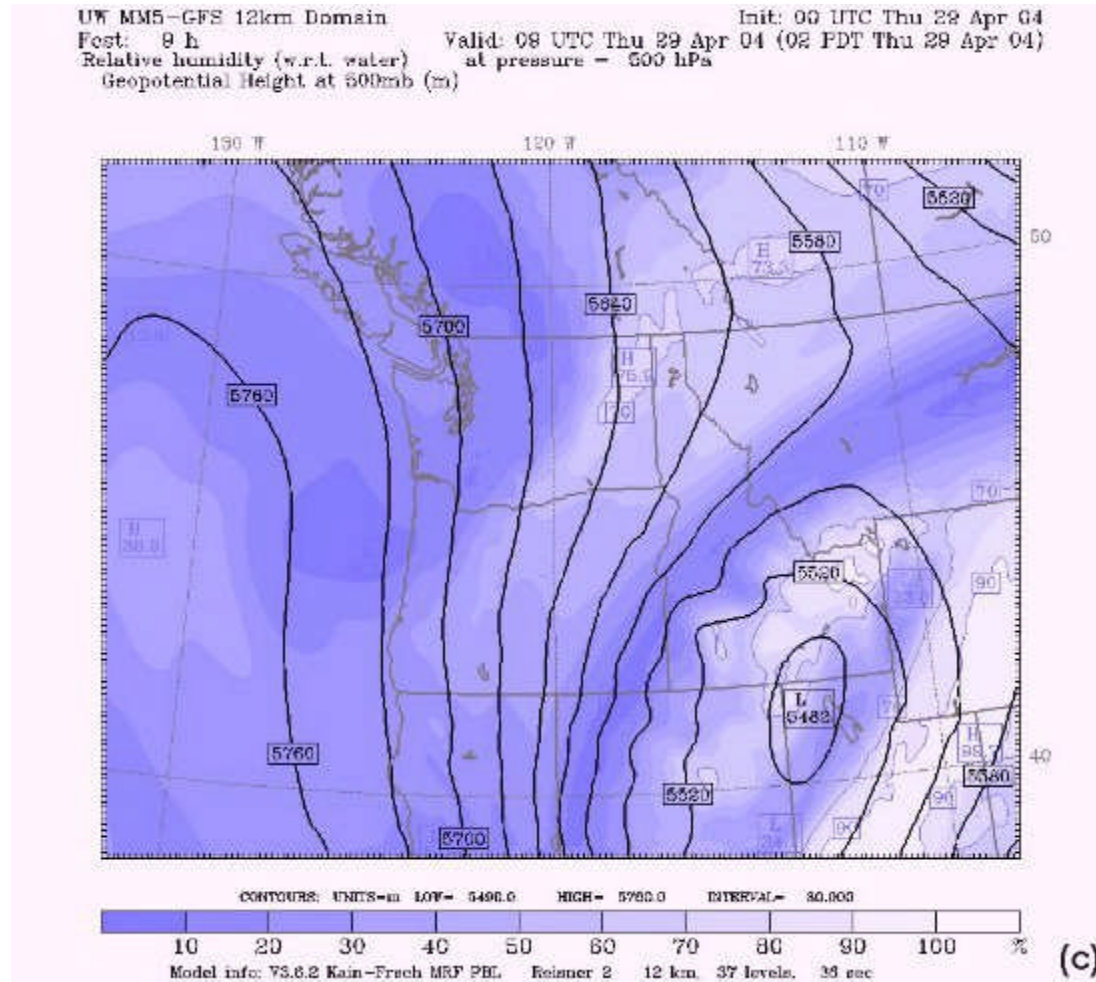
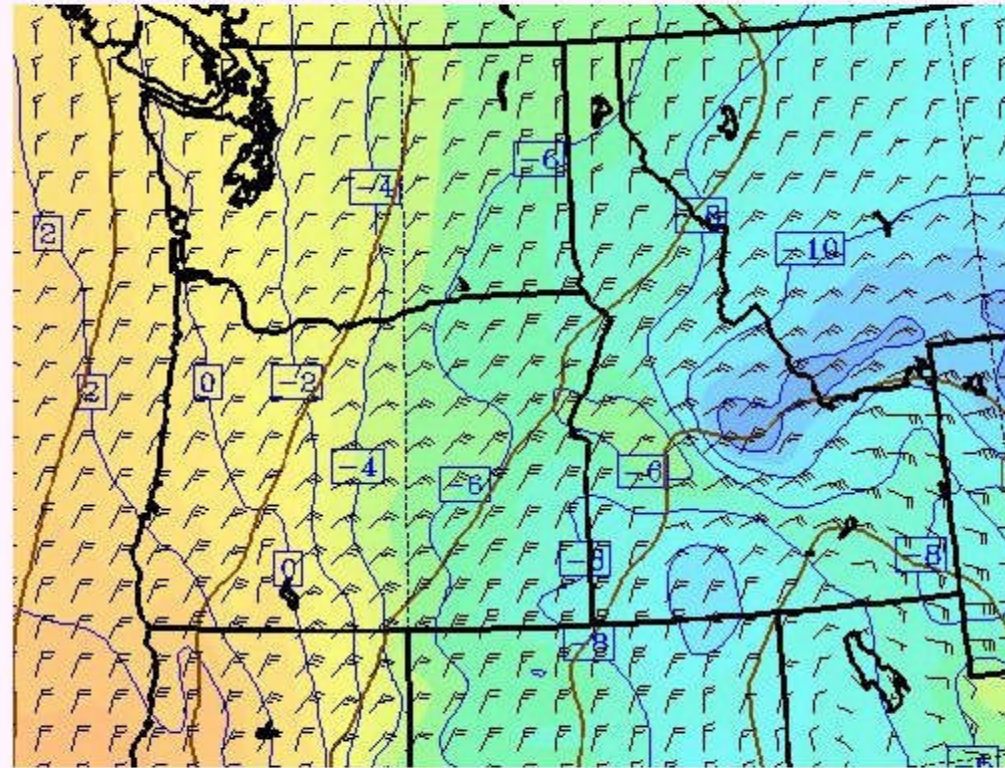


Figure 5: (a) MM5-GFS 300 mb wind speed ( $\text{m s}^{-1}$ ), temperature ( $^{\circ}\text{C}$ ), geopotential height (m), and wind (kt)  
 (b) MM5-GFS 500 mb absolute vorticity ( $\text{s}^{-1}$ ) and geopotential height (m)  
 (c) MM5-GFS 500 mb relative humidity (%) and geopotential height (m)  
 (d) MM5-GFS 700 mb relative humidity (%) and geopotential height (m)

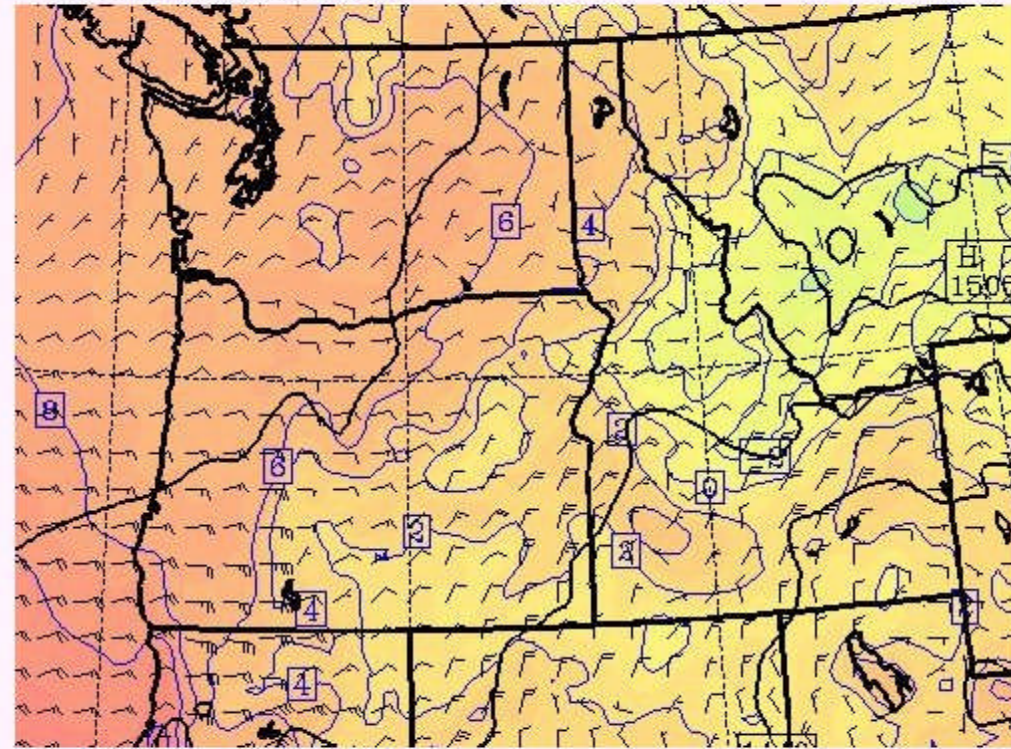


UW MM5-GFS 12km Domain Init: 00 UTC Thu 29 Apr 04  
 Post: 9 h Valid: 09 UTC Thu 29 Apr 04 (02 PDT Thu 29 Apr 04)  
 Temperature at 700mb (°C)  
 Geopotential Height at 700mb (m)  
 Wind at 700mb (full barb = 10kts)



(a)

UW MM5-GFS 12km Domain Init: 00 UTC Thu 29 Apr 04  
 Post: 9 h Valid: 09 UTC Thu 29 Apr 04 (02 PDT Thu 29 Apr 04)  
 Temperature at 850mb (°C)  
 Geopotential Height at 850mb (m)  
 Wind at 850mb (full barb = 10kts)



(b)



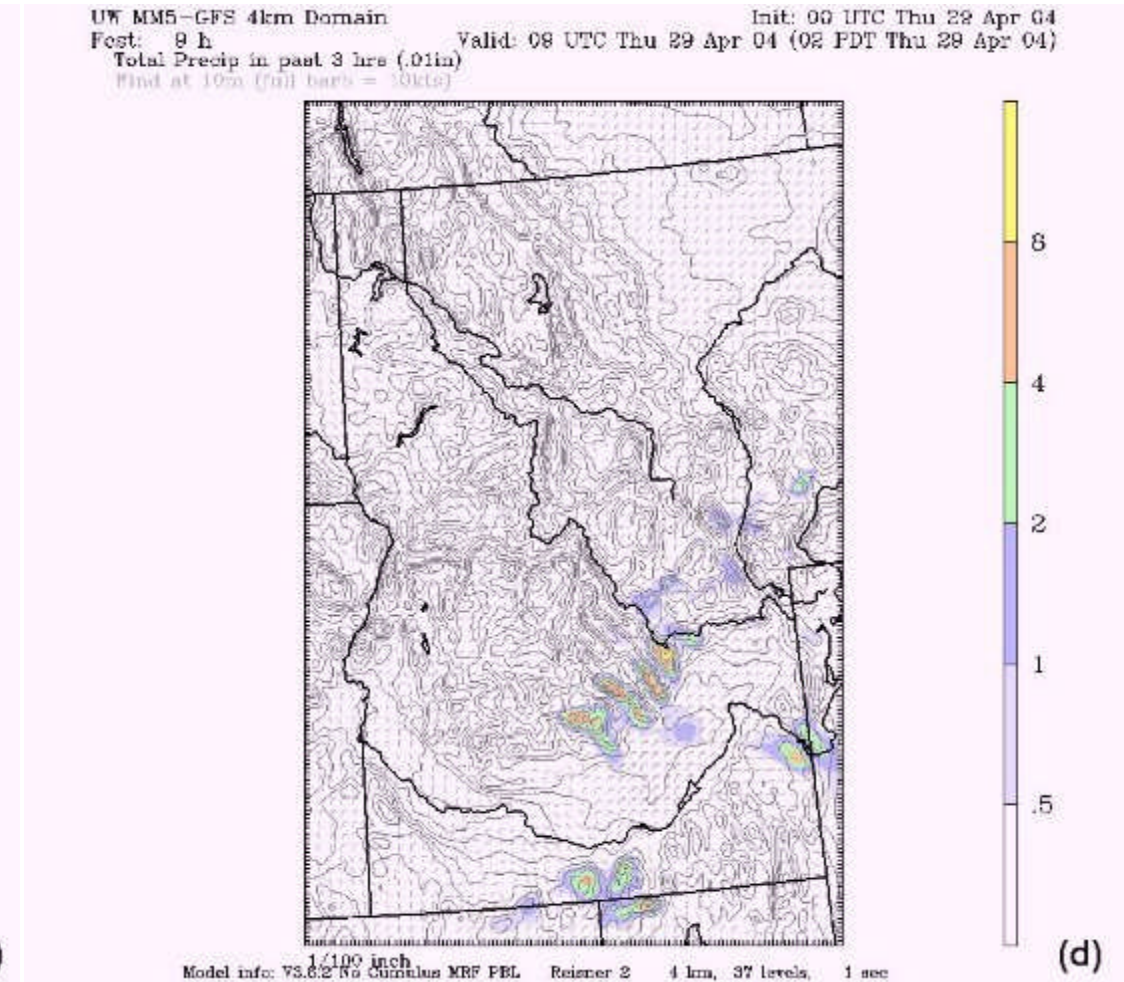
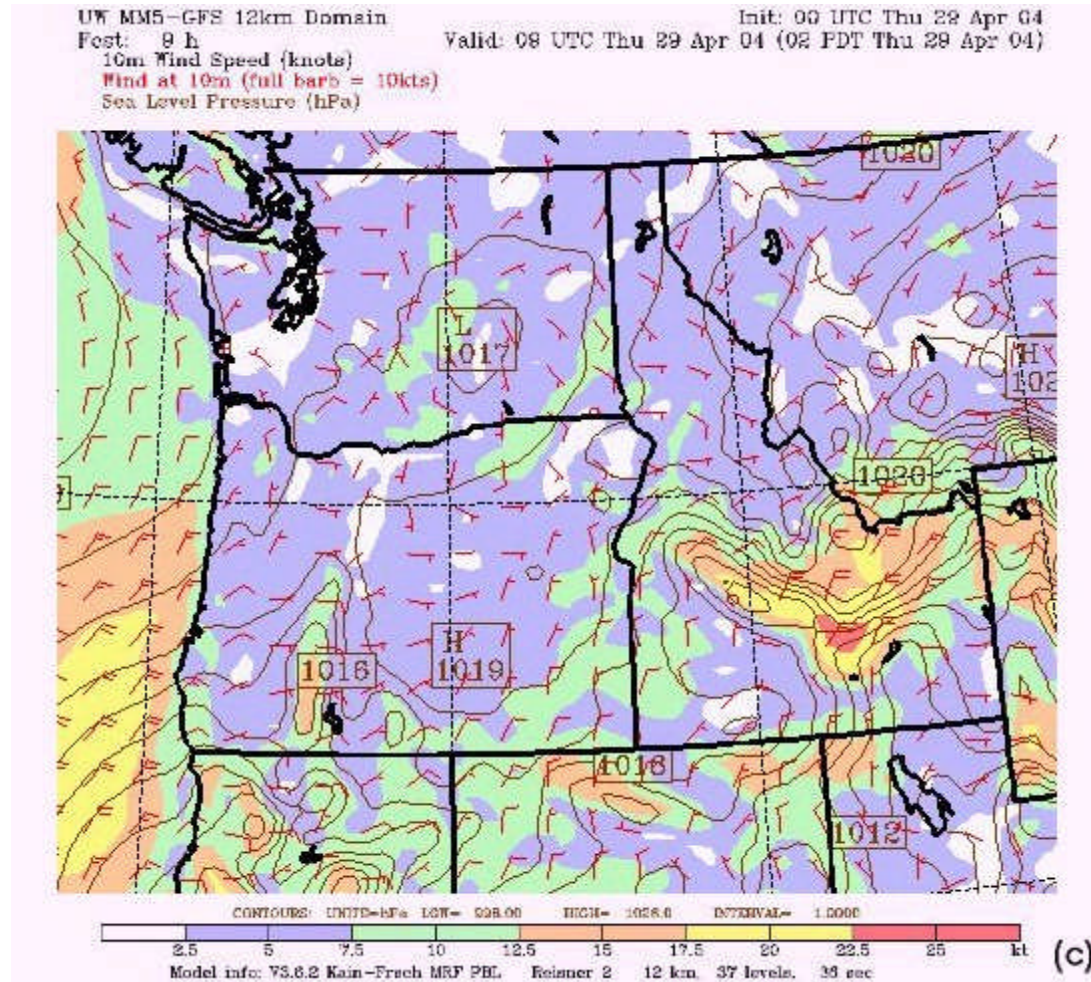
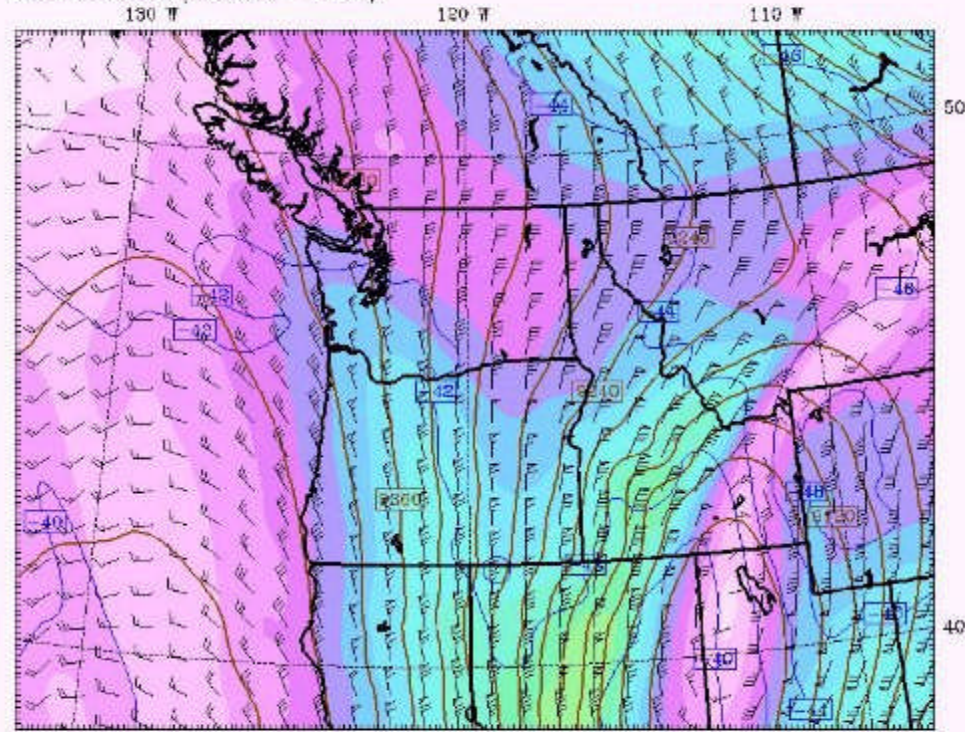


Figure 6: (a) MM5-GFS 700 mb temperature ( $^{\circ}\text{C}$ ), geopotential height (m), and wind speed (kt)  
 (b) MM5-GFS 850 mb temperature ( $^{\circ}\text{C}$ ), geopotential height (m), and wind speed (kt)  
 (c) MM5-GFS 10 m wind speed (kt) and mean sea-level pressure (hPa)  
 (d) MM5-GFS total precipitation in past 3 hours (in) and 10 m wind speed (kt)



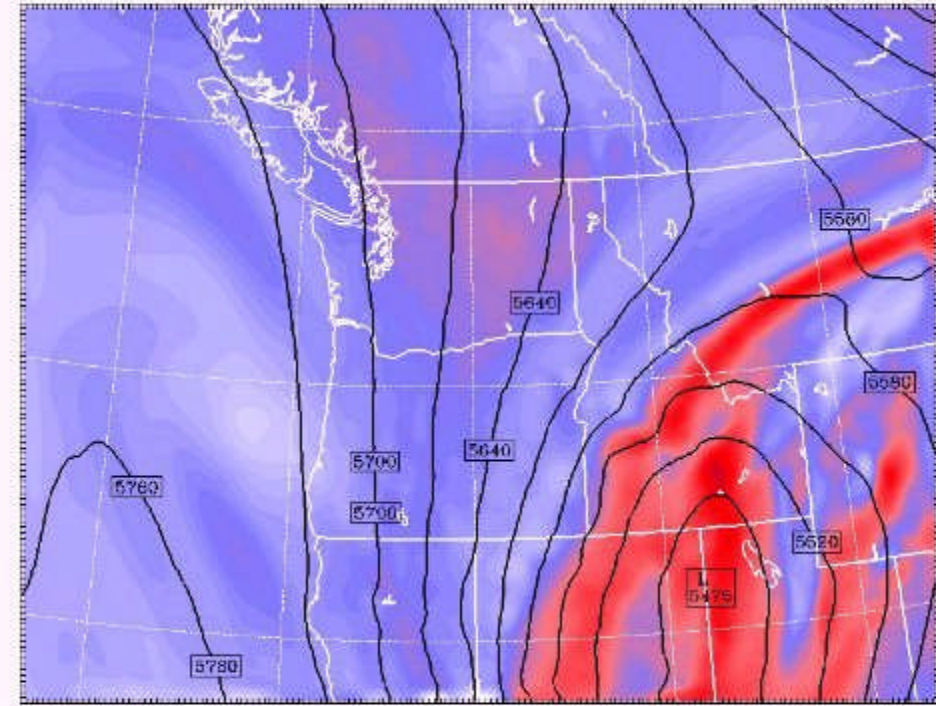
UW MM5-GFS 12km Domain Init: 00 UTC Thu 29 Apr 04  
 Fest: 12 h Valid: 12 UTC Thu 29 Apr 04 (05 PDT Thu 29 Apr 04)  
 300 mb wind speed (m/s)  
 Temperature at 300mb (°C)  
 Geopotential Height at 300mb (m)  
 Wind at 300mb (full barb = 10kts)



CONTOURS: UNITS-m LOV= 9060.0 HIGH= 9450.0 INTERVAL= 30.000  
 CONTOURS: UNITS-°C LOV= -43.000 HIGH= -40.000 INTERVAL= 2.0000  
 Model info: V3.8.2 Kain-Frac MRF PBL Reissner 2 12 km 37 levels 39 sec

(a)

UW MM5-GFS 12km Domain Init: 00 UTC Thu 29 Apr 04  
 Fest: 12 h Valid: 12 UTC Thu 29 Apr 04 (05 PDT Thu 29 Apr 04)  
 Absolute vorticity  
 at pressure = 500 hPa  
 Geopotential Height at 500mb (m)  
 unit = 2



CONTOURS: UNITS-m LOV= 5490.0 HIGH= 5700.0 INTERVAL= 30.000  
 CONTOURS: UNITS-°C LOV= -43.000 HIGH= -40.000 INTERVAL= 2.0000  
 Model info: V3.8.2 Kain-Frac MRF PBL Reissner 2 12 km 37 levels 39 sec

(b)



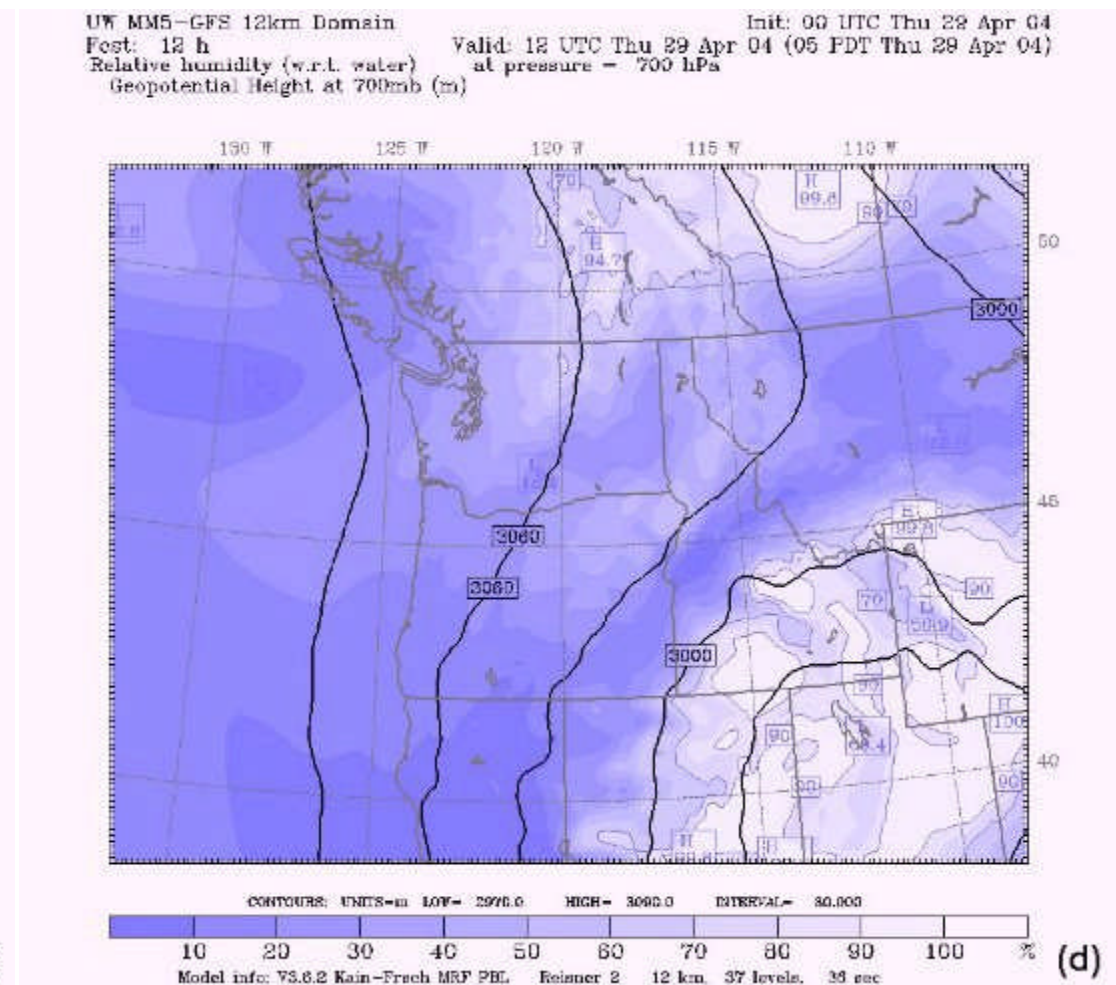
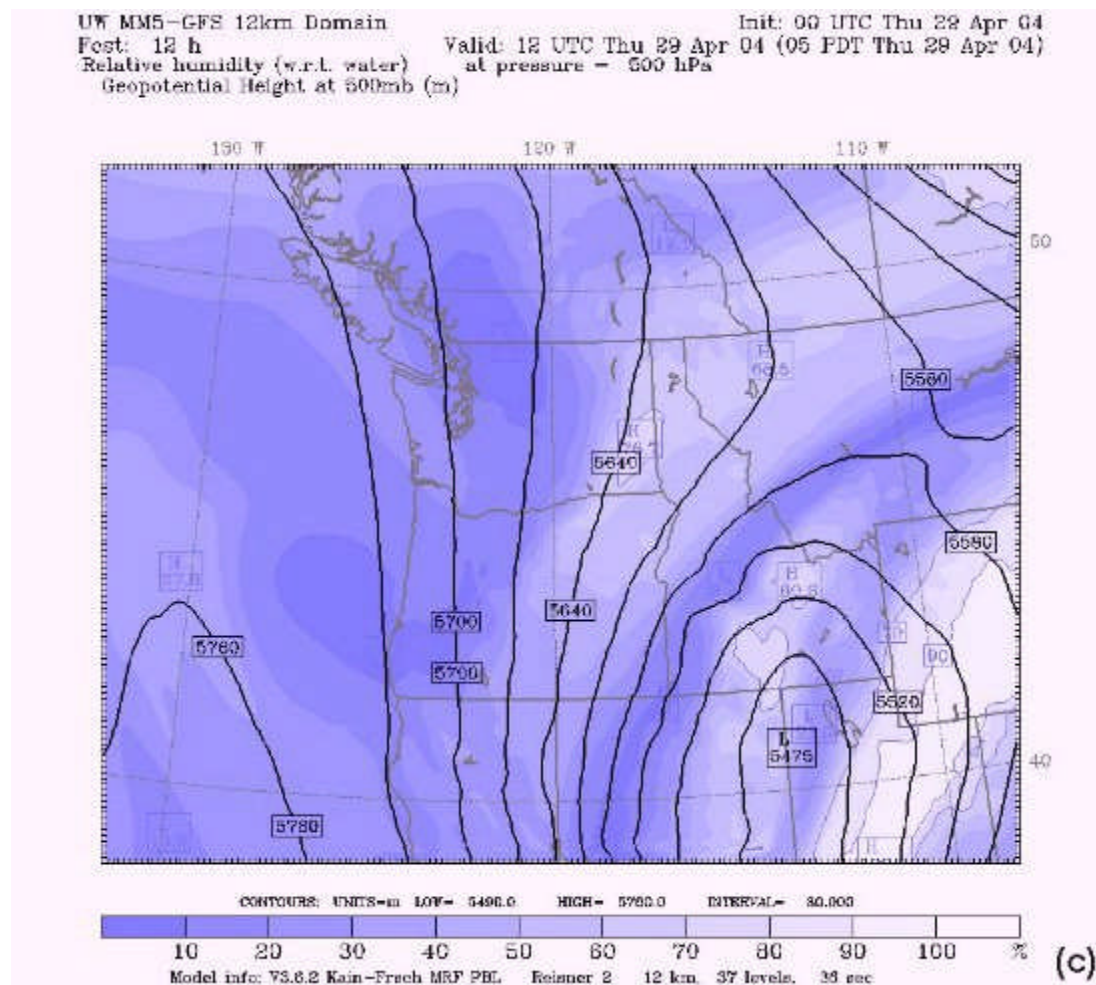
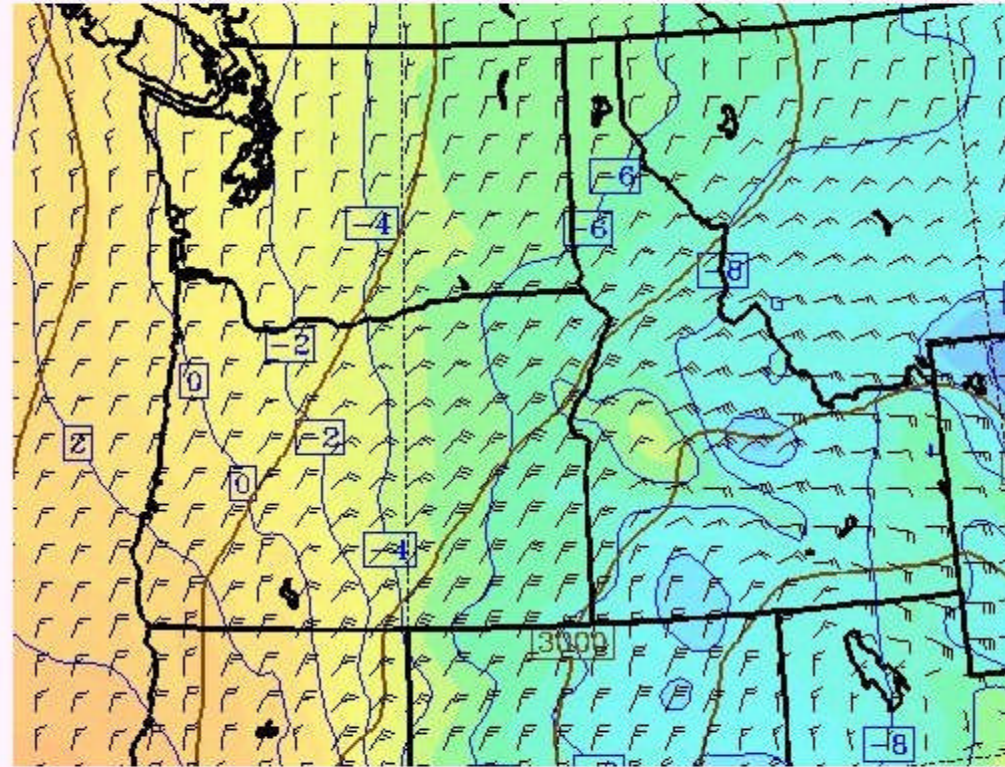


Figure 7: (a) MM5-GFS 300 mb wind speed ( $\text{m s}^{-1}$ ), temperature ( $^{\circ}\text{C}$ ), geopotential height (m), and wind (kt)  
 (b) MM5-GFS 500 mb absolute vorticity ( $\text{s}^{-1}$ ) and geopotential height (m)  
 (c) MM5-GFS 500 mb relative humidity (%) and geopotential height (m)  
 (d) MM5-GFS 700 mb relative humidity (%) and geopotential height (m)



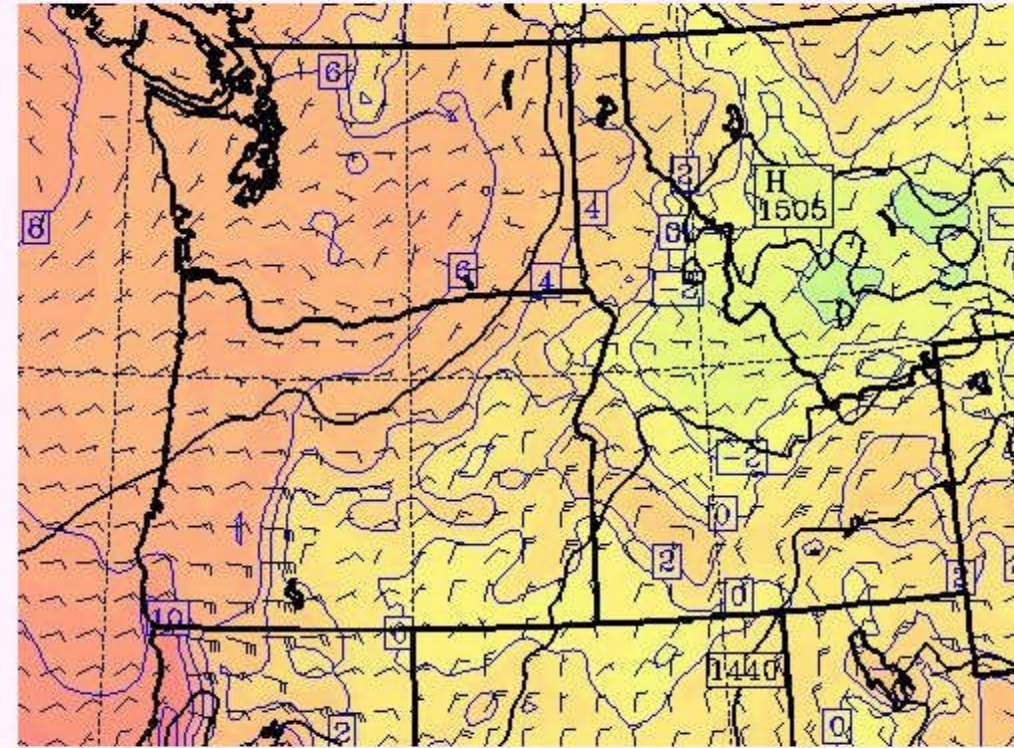
UW MM5-GFS 12km Domain Init: 00 UTC Thu 29 Apr 04  
 Post: 12 h Valid: 12 UTC Thu 29 Apr 04 (05 PDT Thu 29 Apr 04)  
 Temperature at 700mb (°C)  
 Geopotential Height at 700mb (m)  
 Wind at 700mb (full barb = 10kts)



Model info: V3.8.2 Kain-Franch MRF PBL Reisman 2 12 km 37 levels 35 sec

(a)

UW MM5-GFS 12km Domain Init: 00 UTC Thu 29 Apr 04  
 Post: 12 h Valid: 12 UTC Thu 29 Apr 04 (05 PDT Thu 29 Apr 04)  
 Temperature at 850mb (°C)  
 Geopotential Height at 850mb (m)  
 Wind at 850mb (full barb = 10kts)



Model info: V3.8.2 Kain-Franch MRF PBL Reisman 2 12 km 37 levels 35 sec

(b)



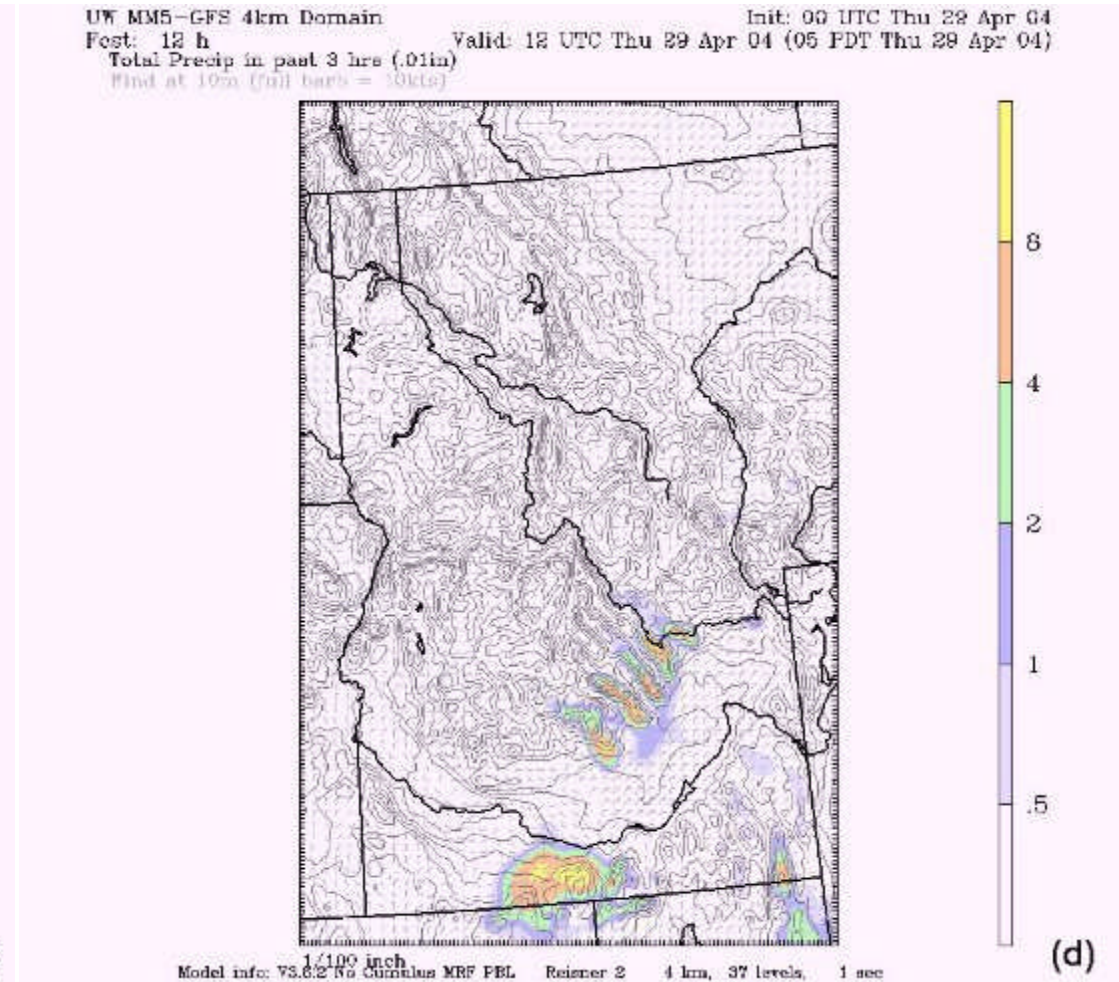
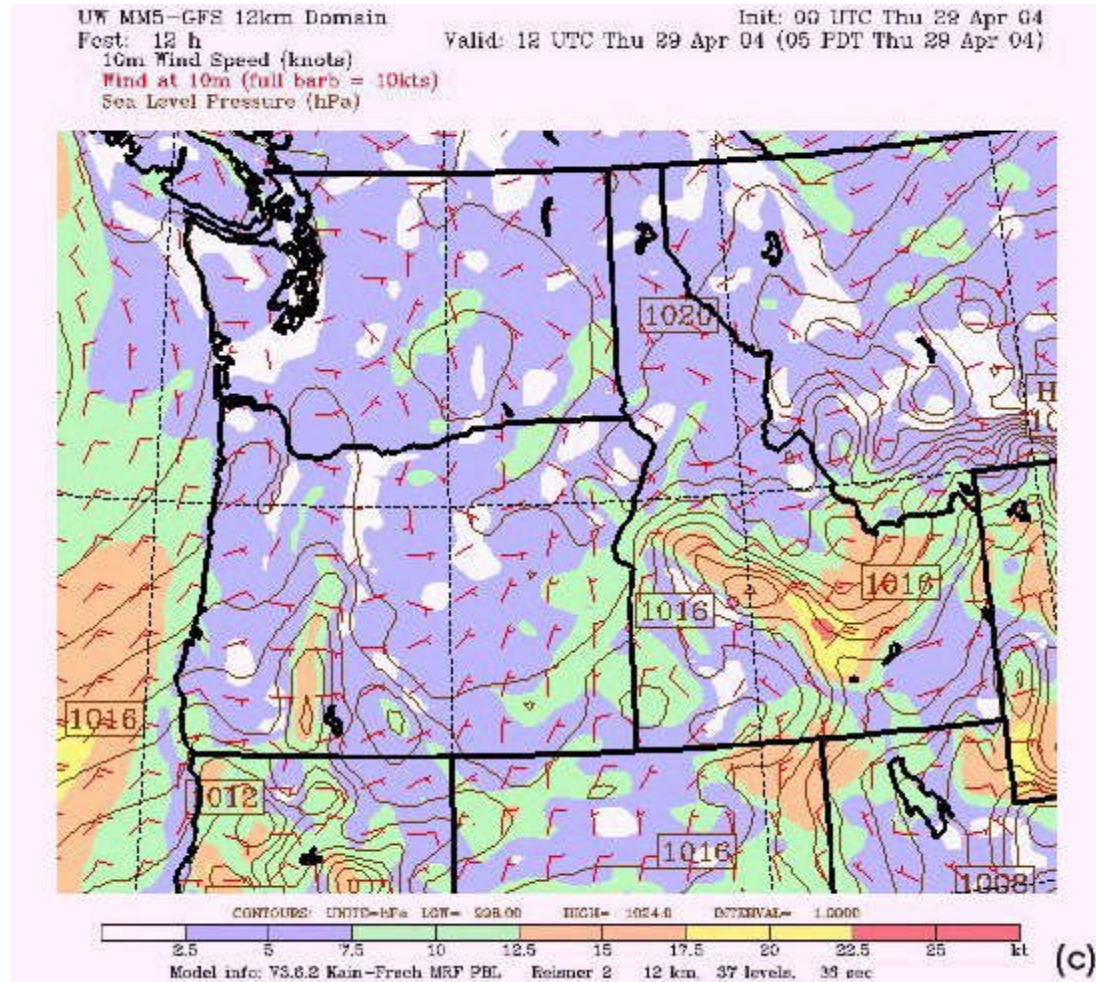
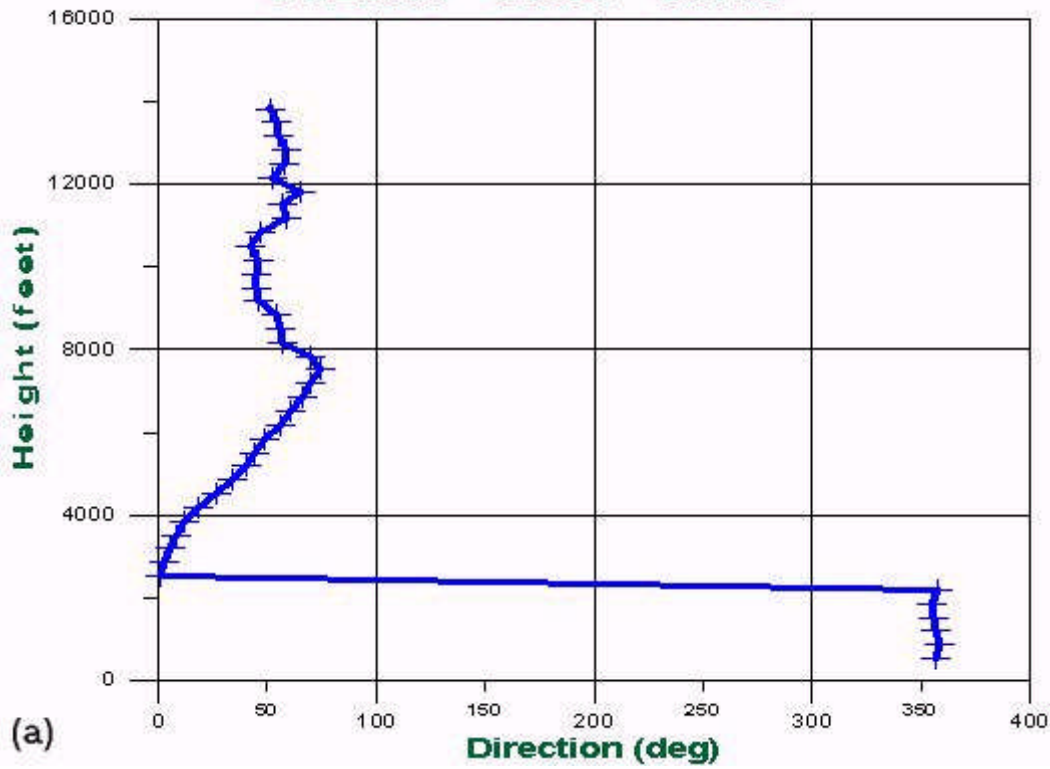


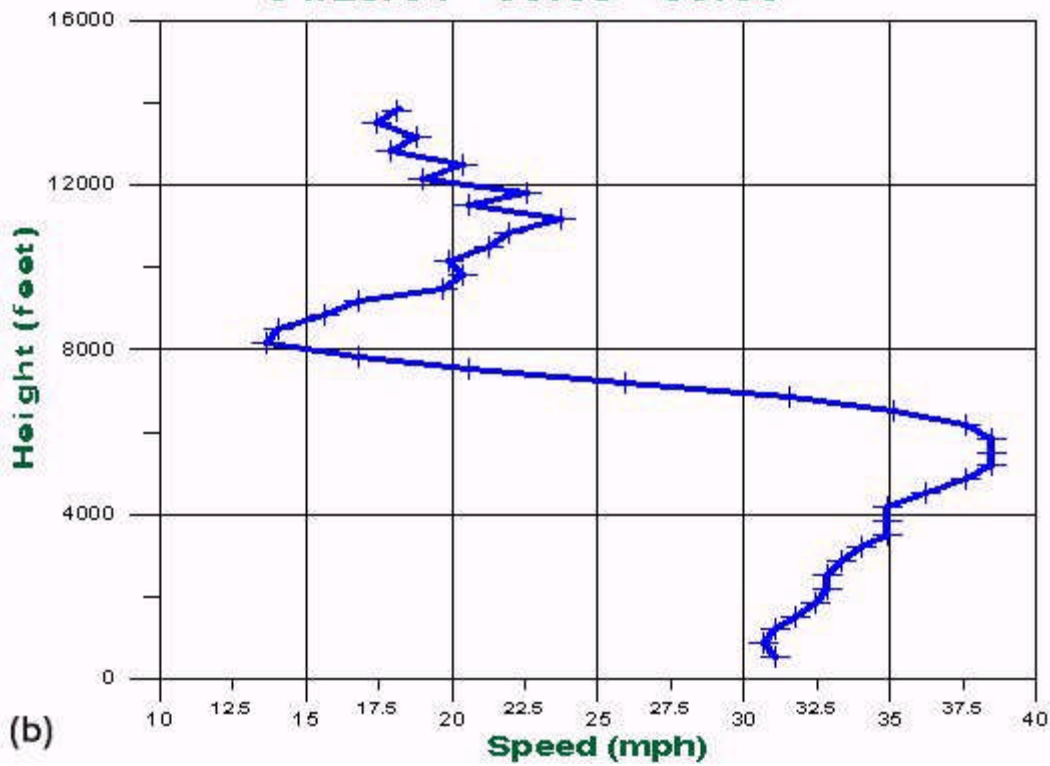
Figure 8: (a) MM5-GFS 700 mb temperature ( $^{\circ}\text{C}$ ), geopotential height (m), and wind speed (kt)  
 (b) MM5-GFS 850 mb temperature ( $^{\circ}\text{C}$ ), geopotential height (m), and wind speed (kt)  
 (c) MM5-GFS 10 m wind speed (kt) and mean sea-level pressure (hPa)  
 (d) MM5-GFS total precipitation in past 3 hours (in) and 10 m wind speed (kt)



04/29/04 00:05 - 00:30

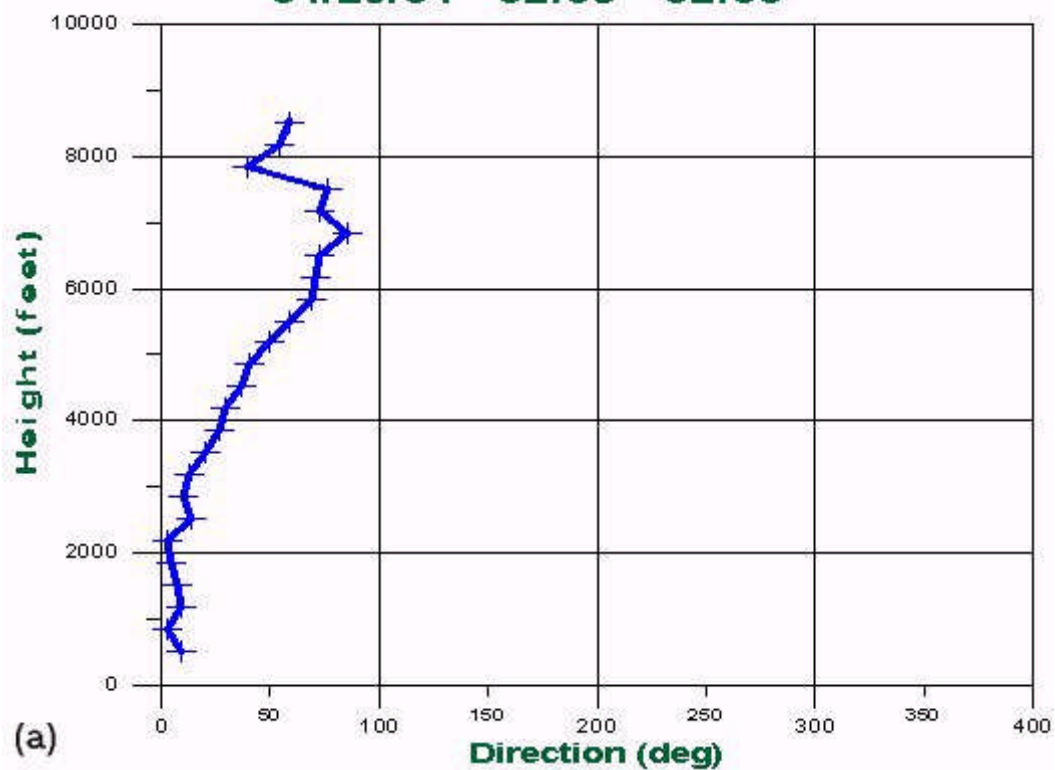


04/29/04 00:05 - 00:30

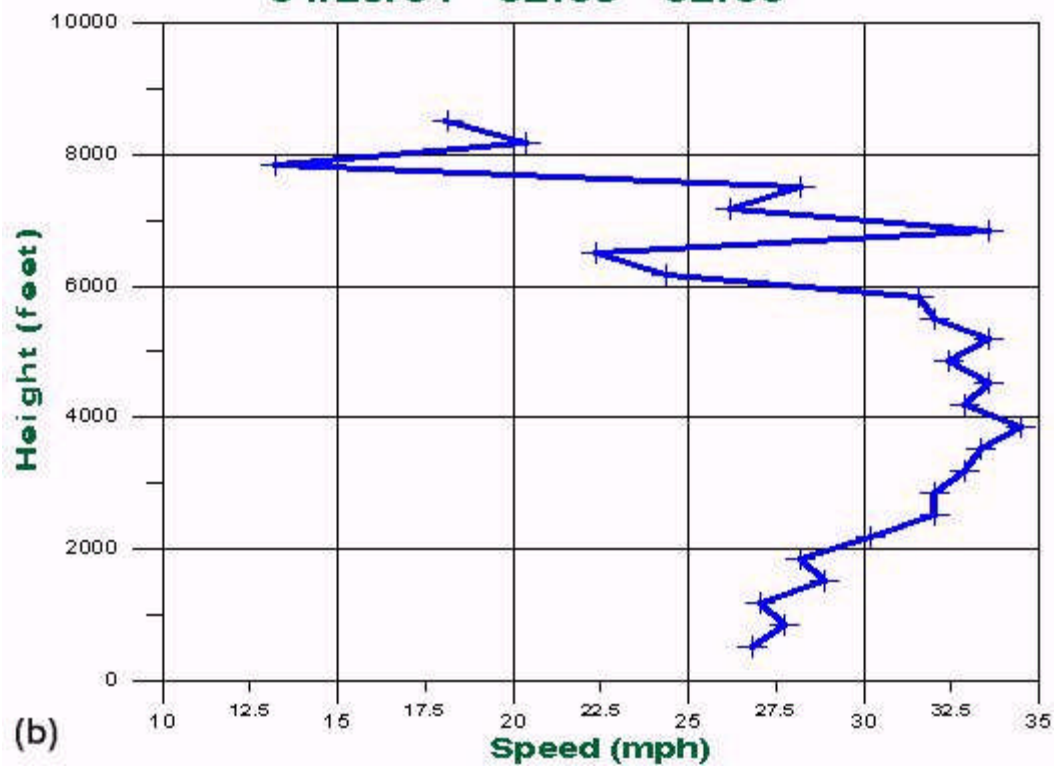




04/29/04 02:05 - 02:30



04/29/04 02:05 - 02:30





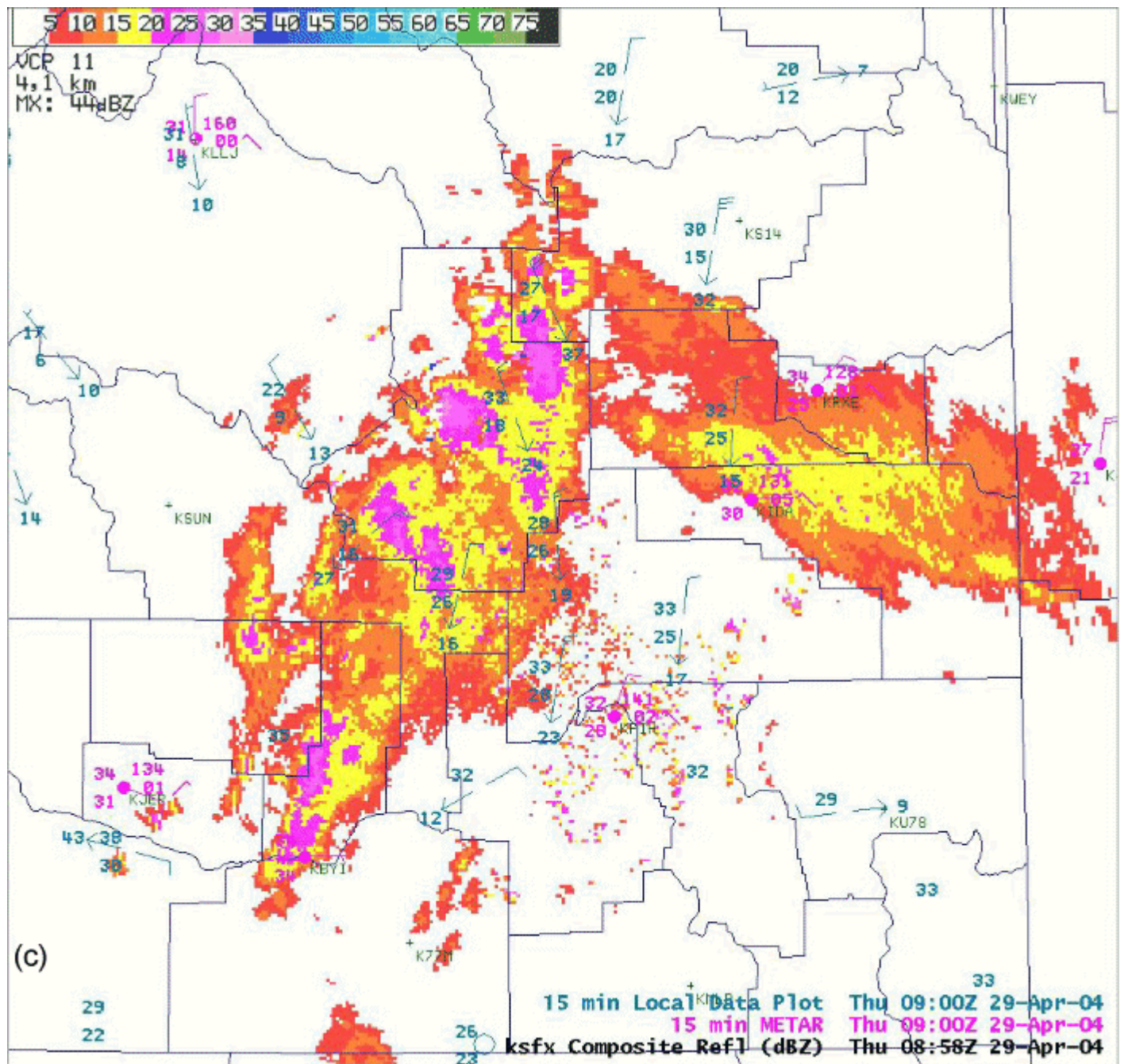
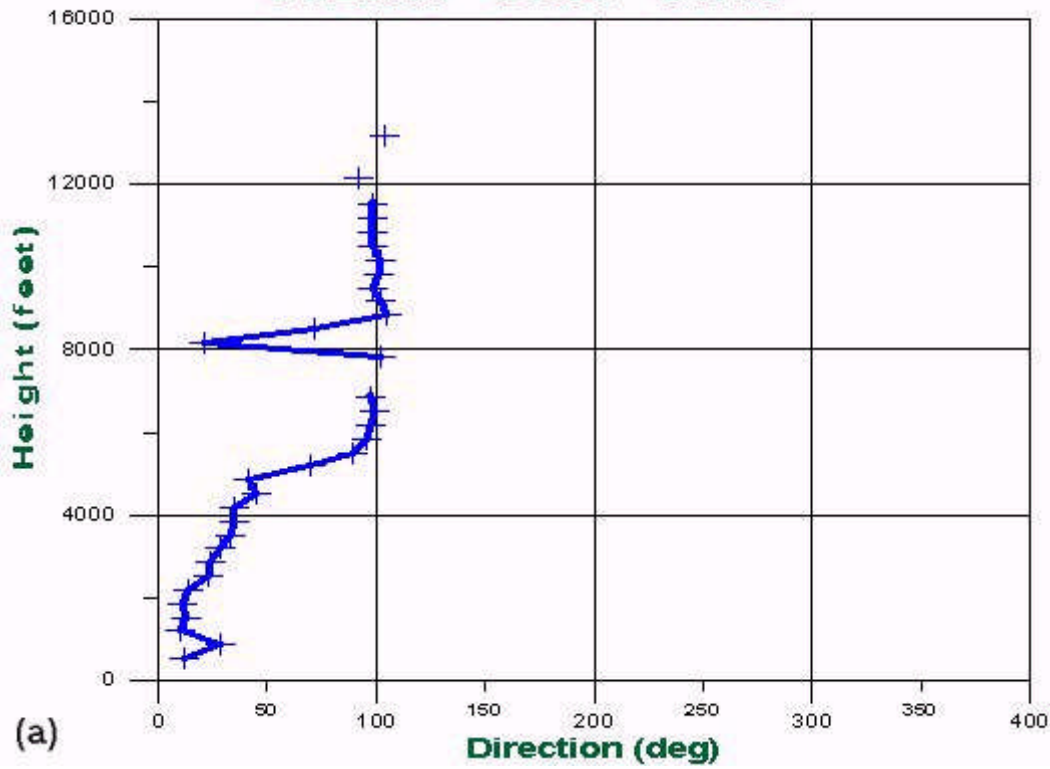
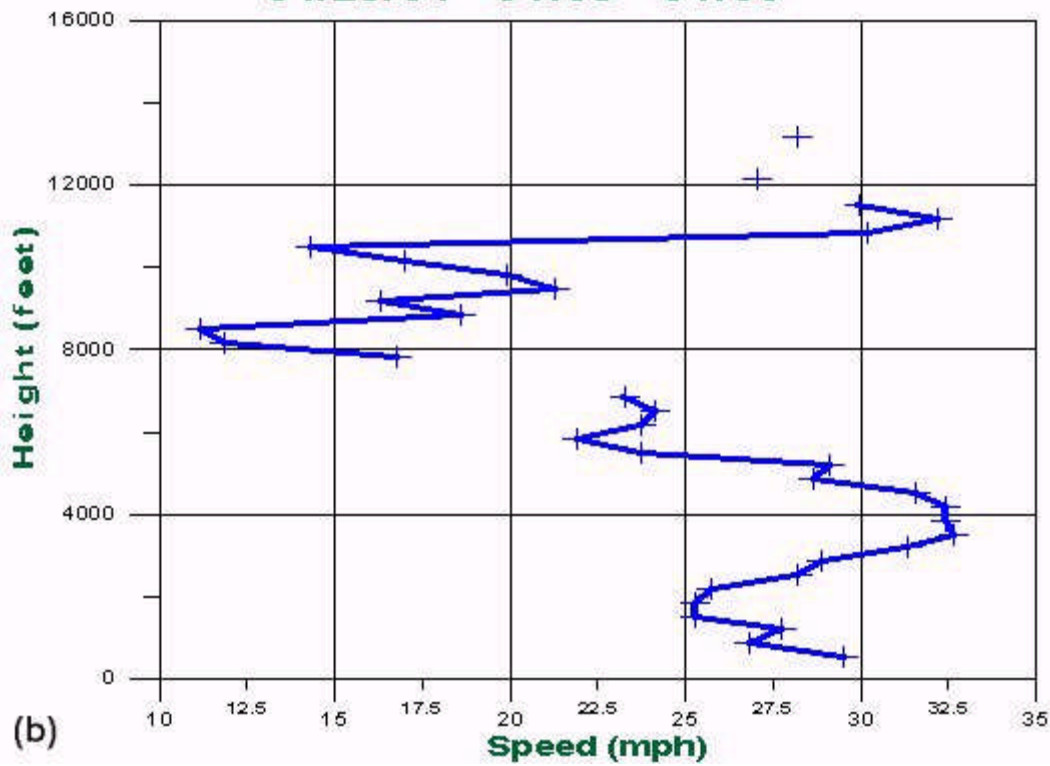


Figure 10: (a) NOAA ARL/FRD Profiler: Wind Direction (degrees)  
 (b) NOAA ARL/FRD Profiler: Wind Speed (mph)  
 (c) NOAA ARL/FRD and NWS METAR observations; WSR-88D KSFx composite reflectivity (dBZ)

04/29/04 04:05 - 04:30



04/29/04 04:05 - 04:30



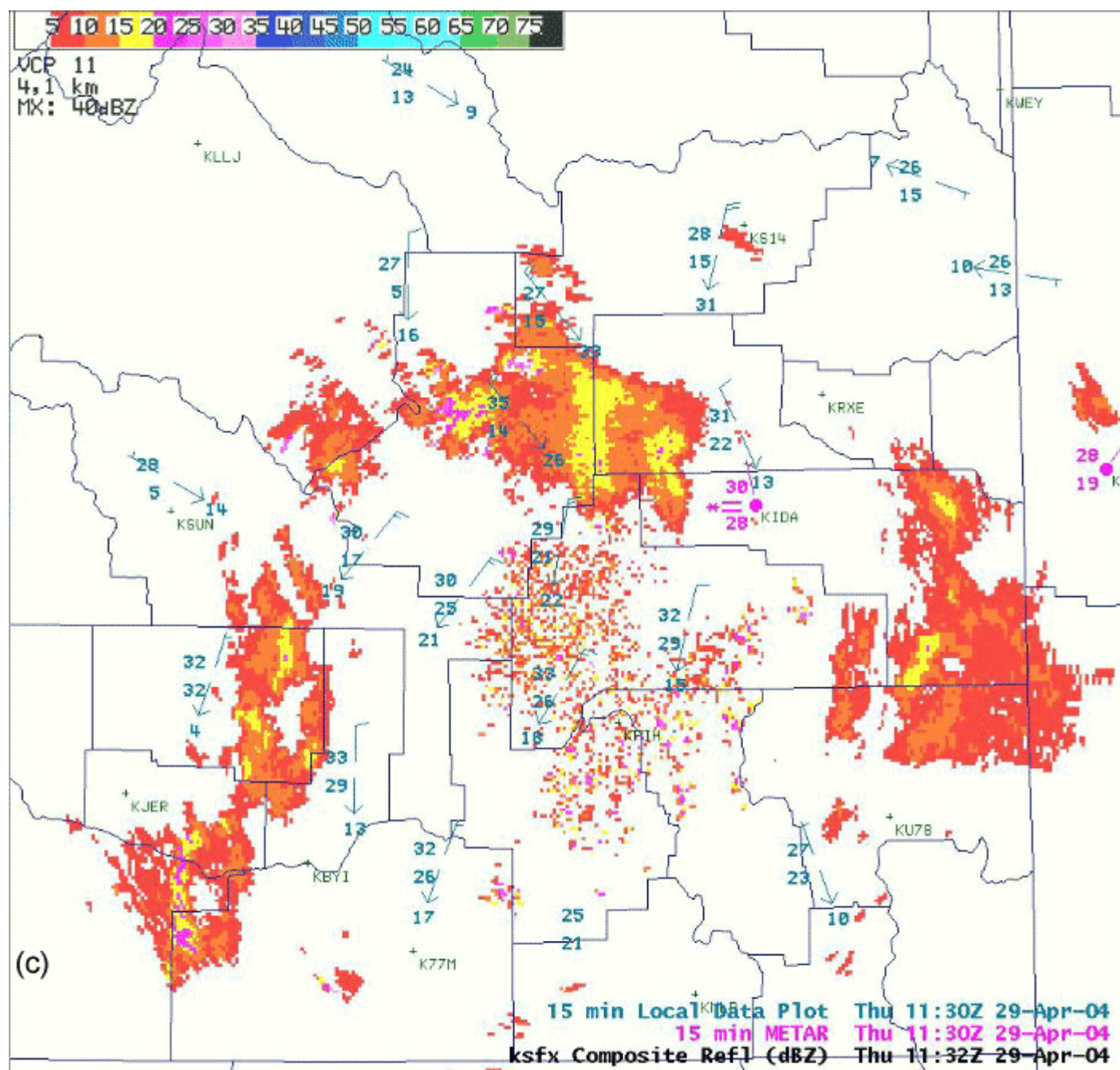


Figure 11: (a) NOAA ARL/FRD Profiler: Wind Direction (degrees)  
 (b) NOAA ARL/FRD Profiler: Wind Speed (mph)  
 (c) NOAA ARL/FRD and NWS METAR observations; WSR-88D KSFx composite reflectivity (dBZ)



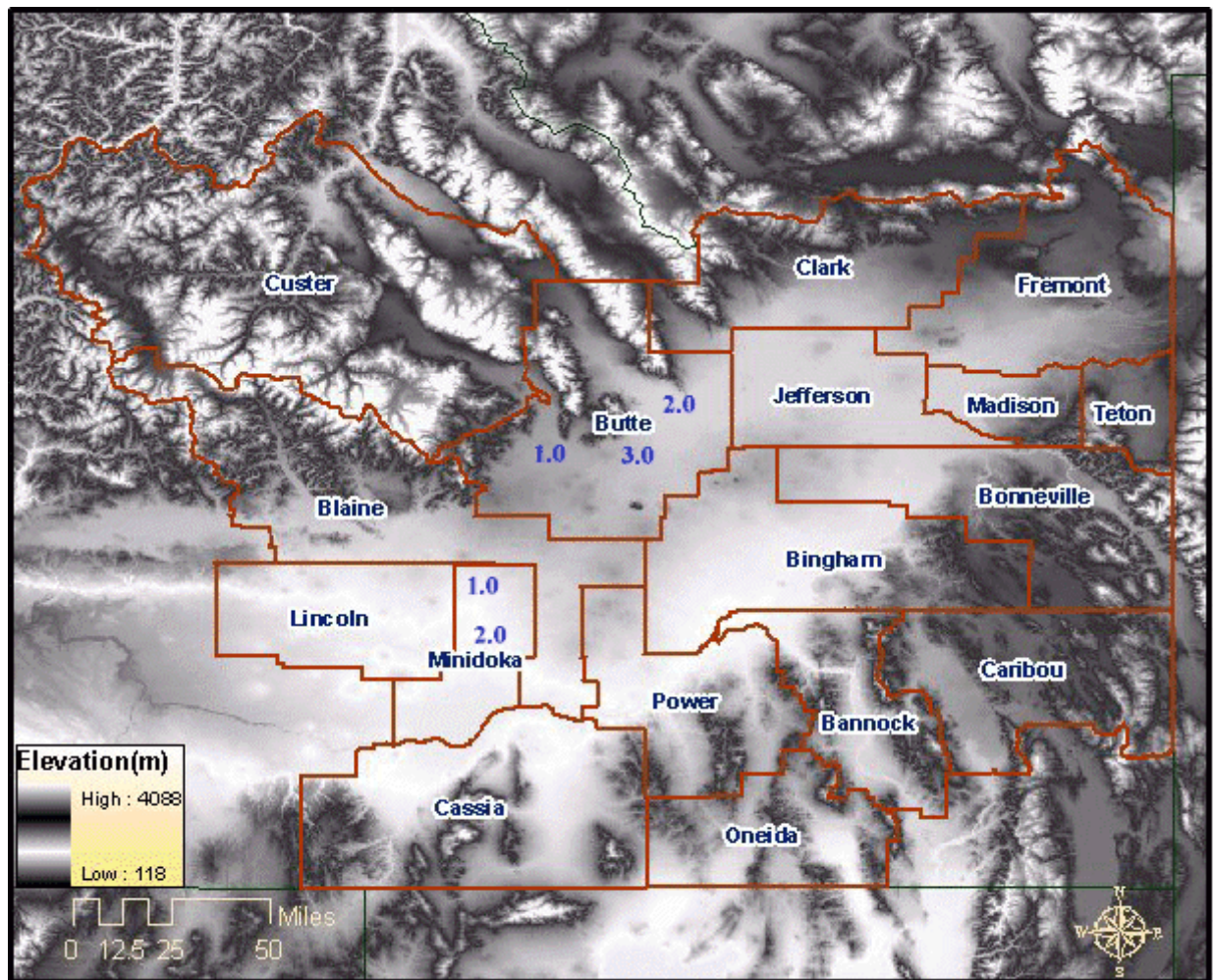


Figure 12: Total observed snowfall (in)